INL/EXT-14-32970
Revision 0

AGR-2 and AGR-3/4 Release-to-Birth Ratio Data Analysis

Binh T. Pham
Jeffrey J. Einerson
Dawn M. Scates
John T. Maki
David A. Petti

September 2014

The INL is a
U.S. Department of Energy
National Laboratory
operated by
Battelle Energy Alliance

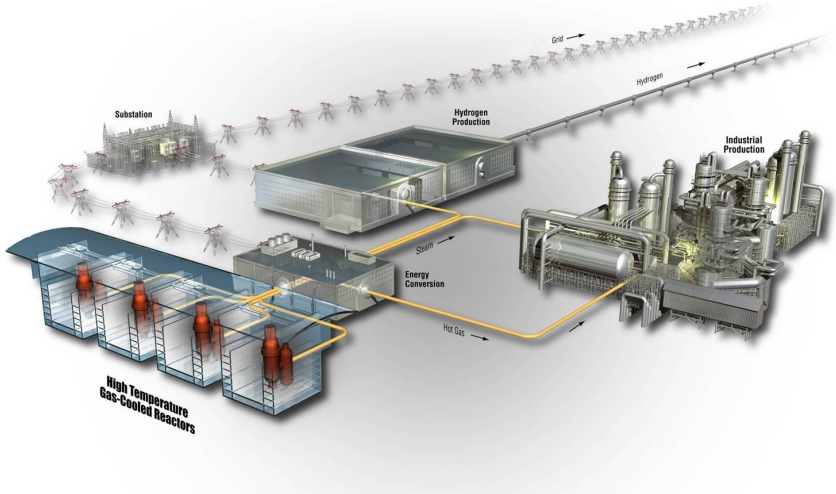

INL/EXT-14-32970
Revision 0

AGR-2 and AGR-3/4 Release-to-Birth Ratio Data Analysis

Binh T. Pham
Jeffrey J. Einerson
Dawn M. Scates
John T. Maki
David A. Petti

September 2014

Idaho National Laboratory
Very High Temperature Reactor Technology Development Office
Idaho Falls, Idaho 83415

http://www.inl.gov

Prepared for the
U.S. Department of Energy
Office of Nuclear Energy
Under DOE Idaho Operations Office
Contract DE-AC07-05ID14517

Very High Temperature Reactor Technology Development Office

AGR-2 and AGR-3/4 Release-to-Birth Ratio Data Analysis

INL/Ext-14-32970
Revision 0

September 2014

Prepared by:

Binh T. Pham Author	Date
Jeffrey J. Einerson Author and NDMAS Technical Lead	Date

Approved by:

David A. Petti VHTR TDO Director	Date
Kirk W. Bailey VHTR Quality Assurance	Date

ACKNOWLEDGEMENT

This work is supported by the High-Temperature Gas-Cooled Reactor Technology Development Office Research and Development Program at Idaho National Laboratory under the U.S. Department of Energy Contract DE-AC07-05ID14517.

SUMMARY

A series of Advanced Gas Reactor (AGR) irradiation tests is being conducted in the Advanced Test Reactor (ATR) at Idaho National Laboratory (INL) in support of development and qualification of tristructural isotropic (TRISO) low enriched fuel used in the High Temperature Gas-cooled Reactor (HTGR). Each AGR test consists of multiple independently controlled and monitored capsules containing fuel compacts placed in a graphite cylinder shrouded by a steel shell. These capsules are instrumented with thermocouples embedded in the graphite enabling temperature control. AGR configuration and irradiation conditions are based on prismatic HTGR technology that is distinguished primarily through use of helium coolant, a low-power-density ceramic core capable of withstanding very high temperatures, and TRISO coated particle fuel. Thus, these tests provide valuable irradiation performance data to support fuel process development, qualify fuel for normal operating conditions, and support development and validation of fuel performance and fission product transport models and codes.

The release-to-birth ratio (R/B) for each fission product isotope (i.e., krypton and xenon) is calculated from release rates in the sweep gas flow measured by the high-purity germanium (HPGe) detectors used in the AGR Fission Product Monitoring System (FPMS) installed downstream from each irradiated capsule. Birth rates are calculated based on the fission power in the experiment and fission product generation models. Thus, this R/B is a measure of the ability of fuel kernel, particle coating layers, and compact matrix to retain fission gas atoms preventing their release into the sweep gas flow, especially in the presence of initially defective particle in AGR-2 and/or the event of particle coating failures that occurred during the AGR-3/4 irradiation. The major factors that govern the transport of fission gases are material diffusion coefficient, temperature, and isotopic decay constant. For each of the AGR capsules, ABAQUS-based three-dimensional, finite-element thermal models are created to predict daily averages of fuel compact temperatures for the entire irradiation period, which are used in establishing the R/B correlation with temperature and decay constant. This correlation can be used by reactor designers to estimate fission gas release from postulated, failed fuel particles in HTGR cores, which is a key safety factor for a fuel performance assessment.

For AGR-1, which was the first AGR irradiation of modern TRISO fuel completed in 2009, there were no particle failures detected. Therefore its irradiation data are not included here. For AGR-2, initially defective particles (or exposed kernels) existed in the fuel compacts based on quality control data. For the AGR-3/4 experiment, particle failures in all capsules were expected due to the inclusion of 20 designed-to-fail fuel particles in each compact, whose kernels are identical to the driver fuel kernels and whose coatings are designed to fail during irradiation. The in-pile particle failures in a capsule are detected using the independent capsule-specific FPMS. The sodium iodide (NaI) scintillation detector-based gross radiation detector has the capacity to detect every fuel particle failure up to and including the first 250 failures from each capsule. As a result, the AGR-2 and AGR-3/4 irradiations provide sufficient R/B data to study fission gas release behavior of TRISO fuel. Also, a few historical irradiations of low enriched uranium carbide/oxide TRISO fuel that had either designed-to-fail particles or had in-pile failures that can provide additional data for comparison to fuel performance data obtained from the AGR-2 and AGR-3/4 irradiations. The

four key irradiations are: (1) HRB-17/18 (General Atomics 1987), (2) COMEDIE-BD1 (Richards 1994), (3) HFR-B1 (ORNL 1994), and (4) HRB 21 (DOE 1995).

AGR 2 irradiation was completed in October 2013 for 559.2 effective full power days. For AGR-2, 190,416 R/B records (mostly in 8 hour intervals) for the 12 krypton and xenon isotopes were received into the Nuclear Data Management and Analysis System database (Pham 2014). However, according to the FPMS data qualification status reported in ECAR-2420 (Scates 2014a) due to the relief valve failure during Cycles 149A and 149B and the capsule flow cross-talk failure that began during Cycle 150B, the FPMS data will not be qualified after the end of Cycle 148B. AGR 3/4 irradiation was completed in April 2014 for 369.1 effective full-power days. A total of 211,524 R/B records for 12 krypton and xenon isotopes were received into the Nuclear Data Management and Analysis System database for AGR 3/4. Contrary to AGR 2, all AGR 3/4 R/B data are qualified because no gas line failures occurred. Of these data, a total of 18,479 values of AGR 3/4 and 2,550 values of AGR 2 daily averaged R/B per failed particle for three selected krypton isotopes (i.e., Kr 85m, Kr 87, and Kr 88) and three selected xenon isotopes (i.e., Xe 135, Xe 137, and Xe 138) were used for this analysis.

To compare the release behavior among the AGR capsules and historic experiments, the R/B per failed particle is used. HTGR designers also use this parameter in their fission product behavior models. To reduce measurement uncertainty of the release rate, the krypton and xenon isotopes selected for regression analysis have a short enough half-life to achieve equilibrium in the capsule, but are also long enough to provide a measureable signal in the FPM detector. For the AGR TRISO fuel, a regression analysis is performed to establish the R/B per failed particle relationship as a function of the isotope decay constant and fuel temperature using AGR-2 and AGR-3/4 irradiation data when fission product release reached equilibrium state. The uncertainty of the estimated number of failed particles in AGR-3/4 capsules is found to have minor impact on the established R/B correlation. This study demonstrates that R/B values for AGR test fuel are comparable to R/B obtained in historic tests. The R/B correlation with isotopic decay constant (or half-life) is very stable with irradiation time, indicating no strong influence of burnup on release.

CONTENTS

FIGURES

TABLES

ACRONYMS

AGR	Advanced Gas Reactor
ATR	Advanced Test Reactor
DTF	designed to fail
EFPD	effective full-power days
FPMS	fission production monitoring system
HTGR	high temperature gas-cooled reactor
R/B	release-to-birth ratio
TC	thermocouple
TRISO	tristructural isotropic
UCO	uranium carbide/oxide
UO_2	uranium dioxide
VHTR	very high-temperature reactor

AGR-2 and AGR-3/4 Release-to-Birth Ratio Data Analysis

1. INTRODUCTION

The fission product behavior of the tristructural isotropic (TRISO)-coated particle fuel is a key factor for performance assessment of very high temperature reactors (VHTRs). The activity of gaseous fission products (such as krypton and xenon isotopes) in the coolant is a direct indicator of fuel performance. The technical basis for VHTR fuel performance and quality requirements needs quantitative assessment of the fission product release (General Atomics 2009). The main sources of release are from the heavy metal contamination in the fuel coatings and graphite matrix material and from defective or failed coated particles (IAEA 1997). A few historical irradiations of low-enriched uranium carbide/oxide (UCO) TRISO fuel were conducted in the 1980s that had either designed-to-fail (DTF) particles or in-pile failures to study fission gas releases from UCO kernels. Since 2006, three Advanced Gas Reactor (AGR) irradiation tests have been conducted in the Advanced Test Reactor (ATR) at Idaho National Laboratory in support of the development and qualification of the U.S. TRISO fuel used in the High Temperature Gas-cooled Reactor (HTGR). Each AGR test consisted of multiple independent capsules containing cylindrical fuel compacts placed in a graphite cylinder shrouded by a steel shell and instrumented with thermocouples (TC) embedded in the graphite, enabling temperature control. AGR configuration and irradiation conditions are based on prismatic HTGR technology distinguished primarily through use of helium coolant, a low-power-density ceramic core capable of withstanding very high temperatures, and coated particle fuel (Petti 2008). Thus, these tests provide valuable irradiation performance data to support fuel process development, qualify fuel for normal operating conditions, and support development and validation of fuel performance and fission product transport models and codes.

For TRISO fuel particles, the release- to-birth ratio (R/B) is a measure of the ability of fuel kernels, particle coating layers, and compact matrix material to retain fission gas species preventing their release into the sweep gas flow. In the absence of particle failure, this ratio is expected to be very low because standard particles within the specification limits (i.e., intact particles with no fabrication defects) are not expected to contribute to the release of fission products under normal operating conditions. The R/B for each of the krypton and xenon isotopes is calculated from release rates measured by the high-purity germanium (HPGe) detectors used in the AGR Fission Product Monitoring System (FPMS) installed downstream from each irradiated capsule. Birth rates are calculated based on the fission power in the experiment and fission product generation models. To compare release behavior among the AGR capsules and between different experiments, the R/B per failed particle is used for the analysis. This parameter is also used in the fission product behavior models within the HTGR research and development program.

For AGR-1, which was the first United State irradiation of modern TRISO fuel and was completed in 2009, there were no in-pile particle failures detected. Thus, AGR-1 R/B data were not included in this analysis. The AGR-2 irradiation can provide data for R/B per failed particle because a few initially defective particles (or exposed kernels) existed in the UCO fuel that was irradiated based on the quality control data (Hunn 2010). For the AGR-3/4 experiment, particle failures in all capsules were expected because of the use of DTF fuel particles whose kernels are identical to the driver fuel kernels but whose coatings are designed to fail under irradiation. There are 80 DTF fuel particles (20 per compact) in each AGR-3/4 capsule, located along the vertical centerline of the fuel compacts. The in-pile fuel failures in each capsule are determined by looking at the temporal profile of the gross gamma counts monitored continuously for each capsule. A fuel particle failure causes the gross gamma activity to peak for a short time higher than normal counts and raises the background activity afterward. This procedure becomes more complicated when multiple particle failures occur at the same time, which can lead to high uncertainty of a number of failures for some capsules. Therefore, the impact of the uncertainty of the number of failed particles on R/B per failed particle is also taken into consideration in this analysis.

Fission produced atoms of the noble gases born in the kernel of failed particles are diffusing through the surrounding materials and swept to the corresponding FPMS detector. The diffusing time depends on the fuel kernel, particle coatings, and compact matrix material properties and temperatures. However, because of the short half-life, radioactive decay reduces most of the noble gas population. It is well documented that under normal operating conditions, the kernel retains more than 95% of the radiologically important, short-lived fission gases (IAEA 1997). For a large number of atoms, the radioactive gaseous depletion rate (or decay constant) is characterized by isotope half-life, during which half of the activated atoms were depleted. These two governing processes (i.e., diffusion and decay) form a basis for formulating a physics-based R/B per failed particle model as a function of fuel temperature and decay constant. In order to reduce R/B measurement uncertainty, krypton and xenon isotopes with short enough half-lifes to achieve an equilibrium condition in the capsule, but long enough to provide measureable signals in the FPMS detector, were selected for the regression analysis. This report describes the regression analysis performed to establish functional relationships between R/B per failed particle of selected noble gas isotopes and temperature for the U.S. TRISO fuel. In addition, the effect of isotopic half-life is obtained from the data. The impact of uncertainty of the estimated number of failed particles in each capsule is also examined. In order to assess the performance of the U.S. TRISO fuel, the R/B per failed particle data in AGR tests will be compared to R/B data obtained in historic tests.

1.1 Purpose and Scope

Fission product release behavior under normal operating conditions is of significant interest in reactor safety analyses. Therefore, for the U.S. TRISO low–enriched uranium fuel, a regression analysis was performed to establish functional relationships between R/B per failed particle of selected noble gas isotopes and temperature using AGR 2 and AGR 3/4 R/B data. This R/B correlation can be used by reactor designers to estimate fission gas release from postulated failed fuel in HTGR cores essential for fuel performance assessment in safety analysis. The fuel irradiation data used for analysis are combined from independently controlled and monitored capsules in the AGR 2 and AGR 3/4 experiments. For each capsule they include the following:

- R/B data for selected krypton and xenon isotopes;
- Number of particle failures;
- Calculated volume-average fuel temperature for AGR-2 and peak fuel temperature for AGR-3/4.

The basis for the qualification status of R/B data is documented by the FPMS technical staff. These documents provide independent verification that the R/B data submitted to Nuclear Data Management and Analysis System meet data collection requirements and conform to NQA-1 (ASME NQA-1-2008 with 1a 2009 addenda) requirements. The AGR thermal analyses provide daily averaged and peak fuel temperatures in each capsule, which are reported in the corresponding documents submitted by the VHTR program modeler.

The R/B data analysis in this report describes the following:

- Technical aspects of fission gas release behaviors, including release model form;
- R/B data used for this analysis, which were captured in the Nuclear Data Management and Analysis System database for AGR-2 and AGR-3/4 irradiations;
- Procedure of in-pile particle failure detection;
- The effect of isotopic decay constant (or half-life) on fission product releases;
- Regression analysis to establish the relationship of fission product gas release as a function of decay constant and fuel temperature, using suitable R/B data from AGR-2 and AGR-3/4 irradiations;
- Comparison between AGR and historical irradiations for fission product gas release from TRISO UCO fuel particles.

2. TECHNICAL APPROACH

2.1 Fission Product Gas Release Model

2.1.1 Fission Product Gas Release

The activity of gaseous fission products in the coolant is a direct indicator of fuel performance. Analyses of fission gas release focuses on the short-lived isotopes of krypton and xenon because these elements are the greatest contributors to the activity in the primary coolant. Standard particles (intact particle without fabrication defects in coating layers) within the specification limits are not expected to contribute to the release of fission products under normal operating conditions (IAEA 1997). This is because under normal operating conditions, the kernel retains more than 95% of the radiologically important, short-lived fission gases such as Kr-88 and the silicon carbide layer (SiC) is considered to be impermeable to most fission products except for some metallic species at high temperatures (General Atomics 2009, Martin 1993).

The heavy metal contamination in the fuel graphite and initially defective/failed particles (typically referred to as an "exposed kernel") are the main sources of fission gas releases. Fission produced atoms of the noble gases released from the kernel of failed particles are diffusing through the cracks in the failed particle coatings into the surrounding materials and then reach the sweep gas flow. This is because the damaged coatings provide no effective resistance to gas release from the kernel. Several processes are involved in the release of fission gas from kernels. The gas atoms diffuse to the grain surfaces, where they accumulate in the porosity and form bubbles, and are finally released by bubble migration and interconnection of the porosity (Martin 1993). The diffusing time depends on the fuel kernel properties and temperatures. On the other hand, radioactive decay reduces their releases into the sweep gas flow. The radioactive gaseous depletion rate (or decay constant) is characterized by isotope half-life, during which half of the activated atoms are depleted. The R/B for a noble gas isotope is used to characterize the performance of the modern U.S. fabricated TRISO coated fuel particles. The two governing processes, diffusion and decay, form a basis to formulate a physics-based R/B per failed particle model as a function of fuel temperature and decay constant. Details of these physical processes and fission product gas release models are discussed in following subsections.

2.1.2 Diffusion of Fission Gas

Fission produced atoms of the noble gases born in the kernel of failed particles are diffusing through the surrounding materials such as fuel kernel, coating layers, and compact matrix. Figure 1 shows the principal release barriers in an HTGR radionuclide containment system. For the TRISO-coated fuel particle, the fuel kernel itself is the main barrier to fission product releases due to its solid structure (i.e., volume diffusion or condensed-phase diffusion). The second barrier to fission product release is the particle coatings, particularly the silicon carbide layer. The fuel compact matrix and fuel-element structural graphite are relatively porous and provide little holdup of the fission gases, which are released from the fuel particles (i.e., grain boundary diffusion or Knudsen and bulk diffusion for noble gases).

For an intact, coated fuel particle, fission product species are mostly contained within its coatings, and releases are insignificant. By contrast for a coated fuel particle with a coating failure (e.g., exposed kernel due to a damaged second barrier), a fraction of the fission gas releases from the kernel are able to penetrate through the cracks (or opening) in coating layers because gas phase diffusion through cracks become the dominant transport mechanism. These fission gases then diffuse through the graphite matrix with much less obstruction and are released into the sweep gas flow. The diffusion coefficient depends mainly on the fuel kernel properties (size and density) and temperatures. The temperature dependence of the diffusion coefficient is usually expressed by the Arrhenius equation:

$$D = D_0 e^{-\frac{E_a}{RT}} \quad , \quad (1)$$

where D_0 is the pre-exponential factor [m^2/J], E_a is the diffusion process activation energy [J/mol], R is the universal gas constant [8.3143 J/(mol K)], and T is the absolute temperature [K].

To characterize release resulting from the diffusion process within a solid spherical material, such as a fuel kernel, the reduced diffusion coefficient D' (s^{-1}) is used. It is defined as the diffusion coefficient D (m^2/s) divided by the squared "equivalent sphere" diffusion radius, *a* (m):

$$D' = \frac{D}{a^2} \quad . \quad (2)$$

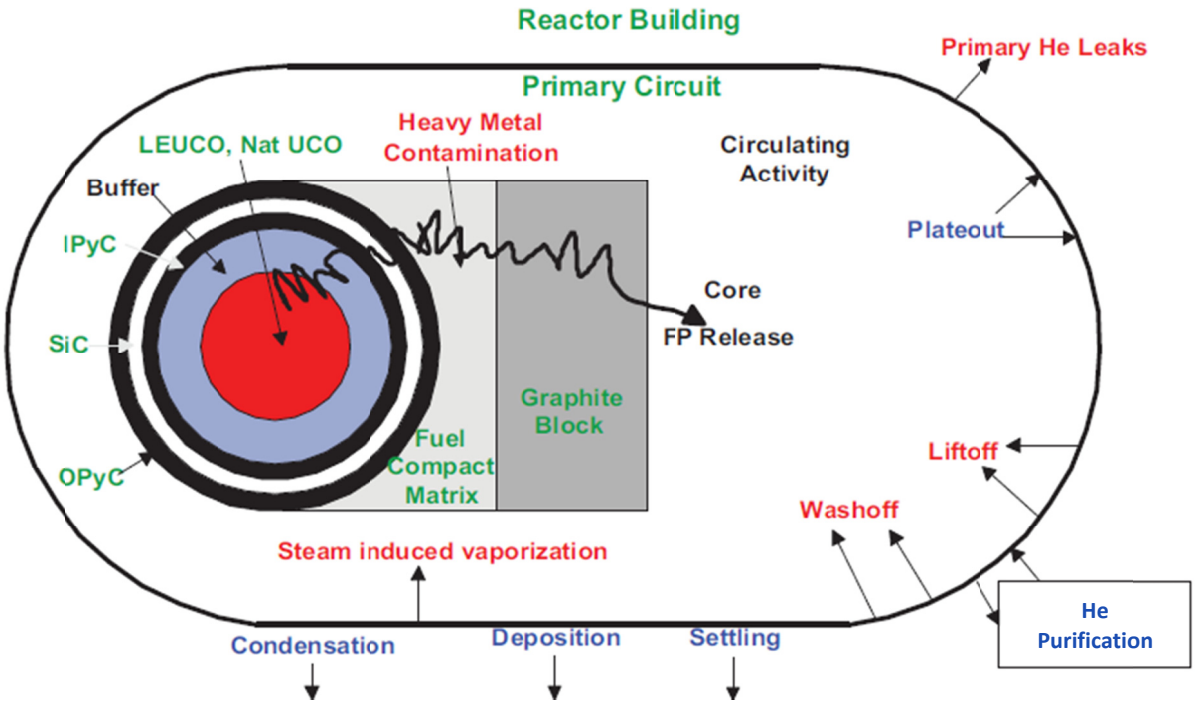

Figure 1. HTGR fission product containment system (General Atomics 2009).

2.1.3 Radioactive Decay of Fission Gas

Radioactive decay is the process by which a nucleus of an unstable atom loses energy by emitting ionizing radiation. Right after birth in a fuel kernel, the fission product isotopic atoms begin depleting over time due to the radioactive decay process. The decay rate for the collection is calculated from the measured decay constants of the nuclides (or equivalently from the half-life). The isotope half-life ($\tau_{1/2}$) is the time taken for the activity of a given amount of a radioactive substance to decay to half of its initial value. The decay rate (or decay constant, λ) is related to the half-life as follows:

$$\lambda = \frac{ln2}{\tau_{1/2}} \quad , \quad (3)$$

2.1.4 Release-to-Birth Ratio Model

Two governing processes (i.e., diffusion and decay) for fission product species transportation from the kernel to sweep gas flow are described in the previous two subsections. R/B for a bare kernel is a function

of the kernel's effective diffusion coefficient, the decay constants of the fission product isotopes, and the surface-area-to-volume ratio, (*3/a*), of a sphere equivalent to the representative grain of fuel with radius *a* (or kernel radius assuming a solid sphere kernel). Under equilibrium conditions when isotope production, radioactive decay, and diffusion from the kernel reach a steady state, the R/B is expressed as (IAEA 1997):

$$R/B = \frac{3}{x}\left(\coth x - \frac{1}{x}\right) \quad , \quad (4)$$

where $x = \left(\frac{\lambda}{D'}\right)^{0.5}$; λ is the decay constant (s^{-1}); D' is the reduced diffusion coefficient (s^{-1}). A similar formula is also presented in reference (ANS 2011).

For short-lived isotopes when $x \gg 1$, then:

$$\frac{R}{B} \approx \frac{3}{x} = 3\sqrt{\frac{D}{\lambda a^2}} \quad . \quad (5)$$

Given experiment specific diffusion coefficient *D* and radius *a* of the fuel kernel, Equation 5 shows the characteristic feature of the $1/\sqrt{\lambda}$ dependence of release for short-lived isotopes. However, when the kernel is surrounded by fuel particle coatings, (which is the second barrier to fission product release) some of the releases from the kernel actually terminate in the remaining coatings. This is known as the recoil effect, which will lower the power of D/λ to less than 0.5. In previous experiments, these values are in a range between 0.1 and 0.5.

Substituting the diffusion coefficient of Equation 1 into Equation 5, the R/B for a TRISO-coated fuel particle can be expressed as a function of fuel temperature and decay constants as:

$$\frac{R}{B} \approx \frac{3}{x} = 3\sqrt[n]{\frac{D_0 e^{-\frac{E_a}{RT}}}{\lambda a^2}} \quad , \quad (6)$$

where instead of using the theoretical value of 0.5, a variable *n* is introduced in the power of D/λ to account for the dependence of release on particle coatings.

2.1.5 Regression Fitting Function

Equation 6 will be used as a basis for the regression analysis to establish the functional relationships of R/B per failed particle for krypton and xenon isotopes with decay constants and temperature for the TRISO-coated fuel. The fission product release model can be derived for R/B per failed particle (R_p) by taking the natural logarithm of Equation 6 and replacing R/B with R_p as:

$$\ln R_p = n \ln\frac{1}{\lambda} + \frac{B}{T} + C \quad , \quad (7)$$

where B is a fuel particle specific constant representing diffusion coefficient dependency on temperature, and C is an irradiation specific constant. This revision helps transform non-linear Equation 6 into the linear form in Equation 7. The regression analysis is performed to best fit this equation to R/B data obtained from AGR irradiations to estimate parameters n, B, and C.

2.2 Release-to-Birth Ratio per Failed Particle Calculation

The two dominant sources of fission product release from the core are as-manufactured heavy-metal contamination and defective/failed coated particles. This is because the intact TRISO fuel particle retains fission gases. Therefore, the R/B per failed particle is a measure of the ability of a fuel kernel and particle coating layers to retain fission gas species, preventing their release into the sweep gas flow in the event of particle coating failures. The compact matrix and graphite component materials do not present much diffusional resistance for these fission gases. For each AGR capsule, the R/B for each of the krypton and xenon isotopes is calculated from release rates measured by the HPGe detectors used in the AGR FPMS and birth rates calculated based on the fission power in the experiment and fission product generation models. The in-pile particle failures during AGR-3/4 irradiation are detected using the independent capsule-specific FPMS. Determination of R/B per failed particle for each of the AGR irradiated capsules is discussed in the following subsections.

2.2.1 Fuel Particle Failures

For AGR capsules, fission gas release comes from three sources: (1) defective exposed kernels, (2) heavy metal contamination, and (3) particle coating failures under irradiation (in-pile failures). The number of initially exposed kernels and heavy metal contamination can be estimated based on failure fractions provided from the fabrication quality control data. According to AGR-1 irradiation, the in-pile failure among qualified fuel particles is not likely.

The in-pile particle failures in a capsule are detected using the independent capsule-specific gross radiation monitor used in the FPMS. The sweep gas carrying fission gaseous species passes in front of the sodium iodide [NaI(Tl)] scintillation detector-based gross radiation monitor. This gross radiation detector has a capacity of detecting every fuel particle failure up to and including the first 250 failures from each capsule. These fuel particle failures are indicated by a rapid rise and drop (or spike) in the temporal profile of the measured gross gamma count rate (as shown in Figure 3). Such spikes are the result of a sudden release of stored fission product inventory inside a just-failed particle. The visual interpretation of the gross gamma data was used to count the number and to record the time of particle failures.

Figure 2 depicts a classic picture of a single particle failure that occurred in AGR-3/4 Capsule 10 on January 19, 2012. Before the failure occurs, the baseline count rate (B_{bf}) is equal to 3,239 counts per second (cps). At the time of failure, the rapid rise (peaking at 13,374 cps) and fall in activity were clearly observed for the event. After the failure, the new baseline count rate (B_{af}) increases to 3,788 cps (549 cps increase relative to before failure), which represents additional release from this failed particle. The release stabilizes after a particle failure in about 4 minutes, which is consistent with what was observed during the NPR-1A experiment (McIsaac 1992). However, detection of in-pile particle failure is not always that simple, especially when there is a partial failure or multiple failures. This occurred during AGR-3/4 irradiation and is described in Section 3.2.1.

2.2.2 Birth Rate

By definition, birthrate of an isotope is the rate of entire production for a specific isotopic atom, even if it is immediately lost to transmutation or decay. Historically, the code, ORIGEN, is generally accepted as the standard for calculating the amount of fission product species across the fuel zone (IAEA 1997). For AGR irradiations, the isotope birthrates in each capsule are calculated from inventory data supplied using the JMOCUP code that links neutronic data computed in Monte Carlo N-Particle (MCNP) to inventory data computed in ORIGEN2.2 (Sterbentz 2014). The birthrates calculation used an ORIGEN2.2 depletion model, assuming no transmutation and decay for krypton and xenon isotopes. The JMOCUP simulation code uses daily averaged values of the ATR operating parameter inputs (such as lobe powers

and control shim cylinder positions) to compute daily birthrates for many fission product isotopes, including krypton and xenon.

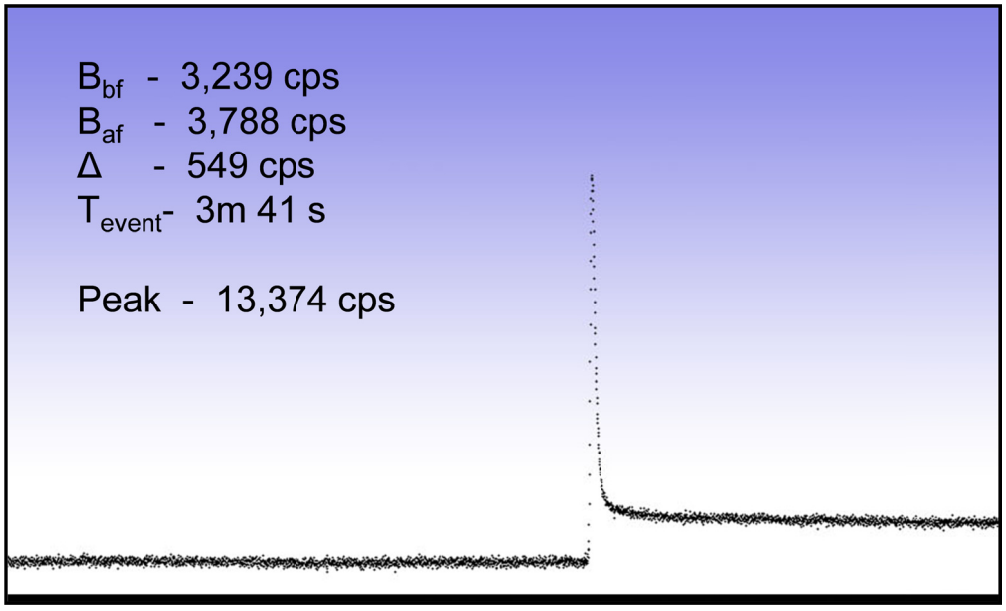

Figure 2. Classic particle failure.

2.2.3 Release Rate

Each capsule has an independent gas line to route its helium/neon gas mixture to transport any fission products released from the capsules to the corresponding FPMS detector by the gas outlet line (Figure 3). The FPMS detector is capable of detecting individual fuel particle failures and providing release rates for the 12 radionuclides as specified in SPC-1345. The summary of FPMS and release data determination for the AGR-1 experiment is given in (Scates 2010). This procedure is also used for all AGR irradiations. Each AGR capsule is continuously and independently monitored by a gross radiation detector and a spectrometer detector in the FPMS installed downstream from the capsule sweep gas line (as shown in the bottom left of Figure 3).

Sweep gas carries released fission product gases from the capsules to the detector system under normal conditions, with a transit time of about 150 seconds. Gas flow passes through a high-purity germanium detector gamma ray spectrometer system. The continuous gamma ray spectrum measurements from the high-purity germanium detectors were used to compute the release activities of several isotopes of krypton and xenon. These measured activities were converted to capsule fission release rates by appropriate correction to account for decay that occurred during transport from the capsules to the detectors. Actual transport times were calculated from outlet gas flow rates and the capsule specific volumes through which samples flow to reach the respective monitoring detector. This conversion formula was derived under the assumption that the equilibrium release conditions were established (Scates 2010). This system provides the fission gas release rate in individual capsules at 8 hour intervals. It also helps detect particle failure under irradiation.

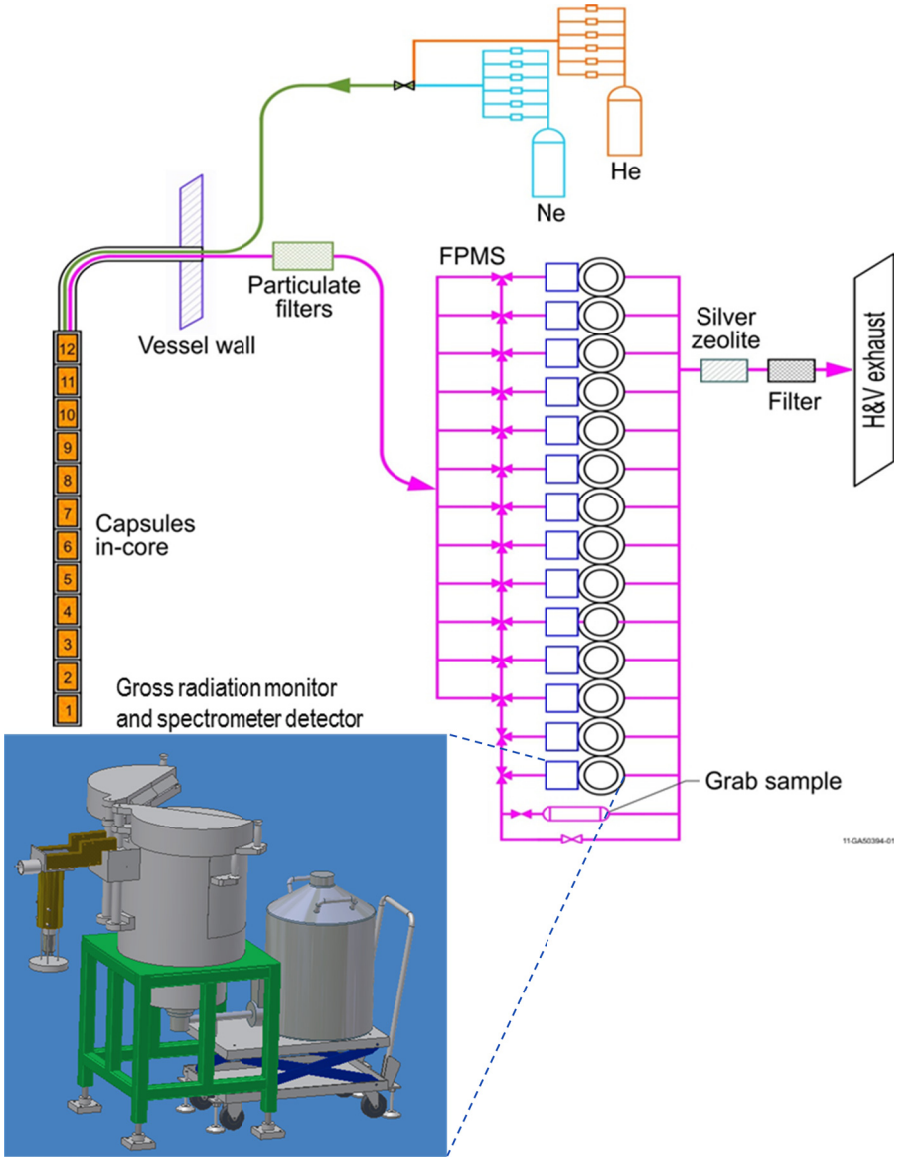

Figure 3. Simplified flow path for AGR-3/4 sweep gas (top) and a gross radiation monitor and spectrometer detector for each AGR capsule (bottom left).

2.2.4 Release-to-Birth Ratio per Failed Particle

The R/B per failed particle is used for this analysis to compare the release behavior among the AGR capsules and historical experiments. For each AGR capsule, assuming the release ratios are the same for all failed particles, the R/B per failed particle for a radionuclide isotope can be calculated as:

$$R_p = \frac{1}{N_f} * \frac{R}{B} \quad , \qquad (8)$$

where R_p is R/B per failed particle; R is the isotope release rate (atom/sec) measured separately for each capsule; B is the isotope birthrate (atom/sec) calculated for each capsule; and N_f is the total number of failed particles in the capsule. The necessary data for determination of R/B per failed particle are birthrate, release rate, and number of failed particles, which are discussed in the previous sections. In reality, the problem of calculating the R/B per failed particle is much more complicated than implied by

Equation 8. This is because the fractional releases from contamination and failed particles vary in space and time.

2.2.5 Release-to-Birth Ratio Uncertainty and Data Selection for Regression Analysis

To reduce measurement uncertainty of the release rate, the krypton and xenon isotopes selected for regression analysis have a short enough half-life to reach equilibrium in the capsule, but are also long enough to provide a measureable signal in the FPMS detector. These isotopes are Kr-85m, Kr-87, Kr-88, Xe-135, Xe-137, and Xe-138.

It is also important that only R/B data captured during capsule equilibrium condition are used for regression analysis. This satisfies the condition of Equation 4 and ensures that the measured release rates at the downstream detector reflect the true release rate in the capsule. During reactor outages, test fuel temperature drops to around 30°C. Subsequently, the diffusion coefficients of the fuel kernel and surrounding material also decrease substantially. Thus, fission product species during this time will accumulate within fuel particles. After reactor startup, fuel temperature rapidly increases to more than 1000°C, allowing accumulated fission products to diffuse out of failed particles into the sweep gas flow. Therefore, during this time, the release rate is higher than at a steady-state condition. The longer outage leads to larger fission product accumulation, which leads to a longer time for the capsule to reach release equilibrium. As a result, data from the first 10 days after long outages between reactor cycles and data from the first 3 days after short outages within a reactor cycle are excluded.

All AGR R/B records are accompanied with measurement uncertainty estimated by the FPMS data generators. They also provide the requirements for storage and display of FPMS data within the Nuclear Data Management and Analysis System database. These requirements prevent the use of data with high-measurement uncertainty in fission product release data analysis. As a result, the negative values and values where uncertainties are greater than 50% are omitted. These data filters remove data from the "short" leadout flow runs or measurements that were incomplete, while leaving other runs that have enough counting statistics unaffected. For example, Table 1 presents uncertainty statistics (i.e., averaged, minimum, and maximum values) of AGR-3/4 R/B data filtered for this analysis. Generally, the R/B measurement uncertainties are lower than 10%. Table 1 also includes decay constants and half-lives of selected krypton and xenon isotopes for reference.

Table 1. AGR-3/4 R/B uncertainty statistics, decay constants, and half-lives for selected krypton and xenon isotopes.

Isotope	Uncertainty* (%)			λ (s^{-1})	Half-life (s)
	Mean	Minimum	Maximum		
Kr-85M	6.1	5.8	38	4.30E-05	16,127
Kr-87	6.0	5.9	9.5	1.52E-04	4,560
Kr-88	5.9	5.8	6.6	6.78E-05	10,223
Xe-135	6.1	5.8	26.3	2.12E-05	32,767
Xe-137	14.1	10.2	17.8	3.01E-03	230
Xe-138	6.8	6.3	8.2	8.19E-04	846

*Only R/Bs with uncertainty less than 50% and a standard 8-hour interval are used.

2.3 Fuel Temperature Calculation

Figure 4 shows a physical sketch representing the thermal model and main parameters of each AGR capsule. The ATR primary cooling water is the ultimate heat sink for each capsule. The fission power predominantly generated in the fuel compact and graphite sample holder is primarily conducted out to the ATR primary cooling water through the two gas gaps: one between the fuel compact and the graphite holder, and a larger one between the graphite holder and the stainless steel shell. The tests are instrumented with TCs embedded in graphite blocks to measure the lower temperature in the graphite. The independently controlled helium-neon gas mixture flows through the control gas gap (this refers to the gap between the graphite holder and the stainless steel shell) to maintain specified TC readings (or a TC set point), ensuring that target fuel temperatures are within the specification defined by program management (SPC-1064).

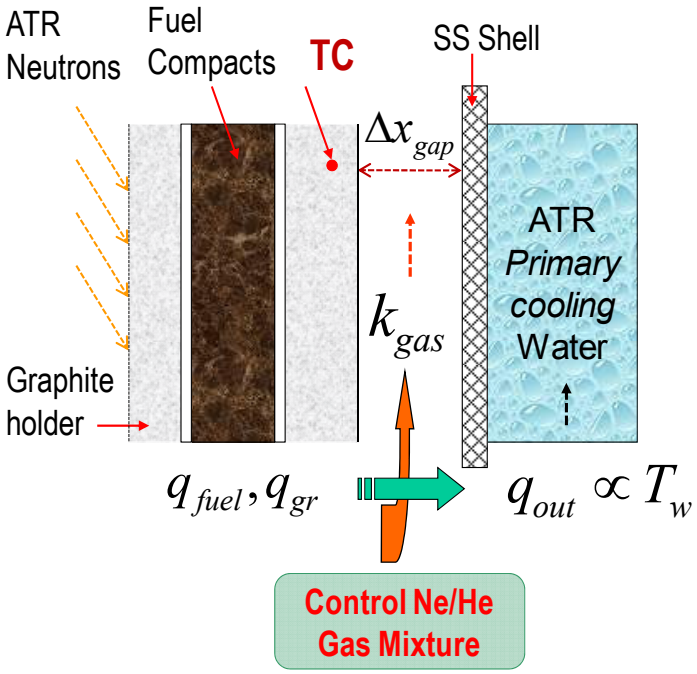

Figure 4. Physical sketch of the axial cut of an AGR capsule.

ABAQUS-based (Version 6.8-2), three-dimensional finite-element thermal models are created for each capsule of the AGR experiments to predict daily averages of fuel compact and TC temperatures for the entire irradiation period when the ATR core is at power. The validation of ABAQUS (version 6.8-2) was reported in (Hawkes 2014). It is comprised of 10 thermal models validating different aspects of ABAQUS' heat transfer abilities. The maximum difference between ABAQUS calculated values and exact theoretical values is less than 2.0%.

The main time-series inputs to the thermal model are daily component (i.e., fuel compacts and graphite sample holder) heat rates and fast neutron fluences calculated from the as-run depletion analysis (Sterbentz 2014) and daily gas compositions of the helium-neon mixture (Ne fraction). The fast neutron fluence is needed for calculation of the components' thermal conductivity and for estimation of the control gas gap changes due to graphite shrinkage. The control gas gaps and compact-graphite holder gas gaps vary based on fast neutron fluence (Hawkes 2014a) due to complex swelling or shrinking of graphite holders and shrinking of fuel compacts. The AGR thermal model assumes that the control gap is evenly and linearly slightly changing over the entire irradiation from initial actual hot gap size (subtracting thermal expansion of the graphite holder) to the estimated end gap. The gas gap changes were estimated based on the dimensional measurements of the AGR-1 irradiated compacts and graphite holders obtained

during post-irradiation examination. These gas gap variation models help improve the agreement between model-predicted and measured TC temperatures. The ABAQUS thermal model uses an approximate 350,000 eight-node hexahedral brick finite element mesh to estimate capsule temperature profiles (as shown in the typical cutaway view of three fuel stacks presented in Figure 5) for one AGR-2 capsule (Hawkes 2014a). AGR-3/4 capsules have only one fuel stack that consists of four compacts; the highest temperatures are along the compact center lines.

Fuel temperature in one capsule can vary spatially for more than 200°C for each time step (in the 750 to 1013°C range [as shown in Figure 5 for the AGR-2 capsule] and in the 827 to 1093°C range [as shown in Figure 6 for the AGR-3/4 capsule]). The temperature of failed particles needed for R/B regression analysis was estimated using this calculated fuel temperature profile. For AGR-2, because location of the defective exposed kernel is unknown and heavy metal contamination is spread throughout the fuel compacts, the "failed particle" temperature was assumed to be equal to volume-averaged fuel compact temperature. For AGR-3/4, the DTF fuel particles were inserted along the center line of each compact, where temperatures are the hottest (Figure 6). Therefore, the failed particle temperature for AGR-3/4 was more likely to be the peak fuel temperature. This assumption might lead to a slightly higher than actual temperature for some DTF particles located on the top and bottom of each AGR-3/4 capsule.

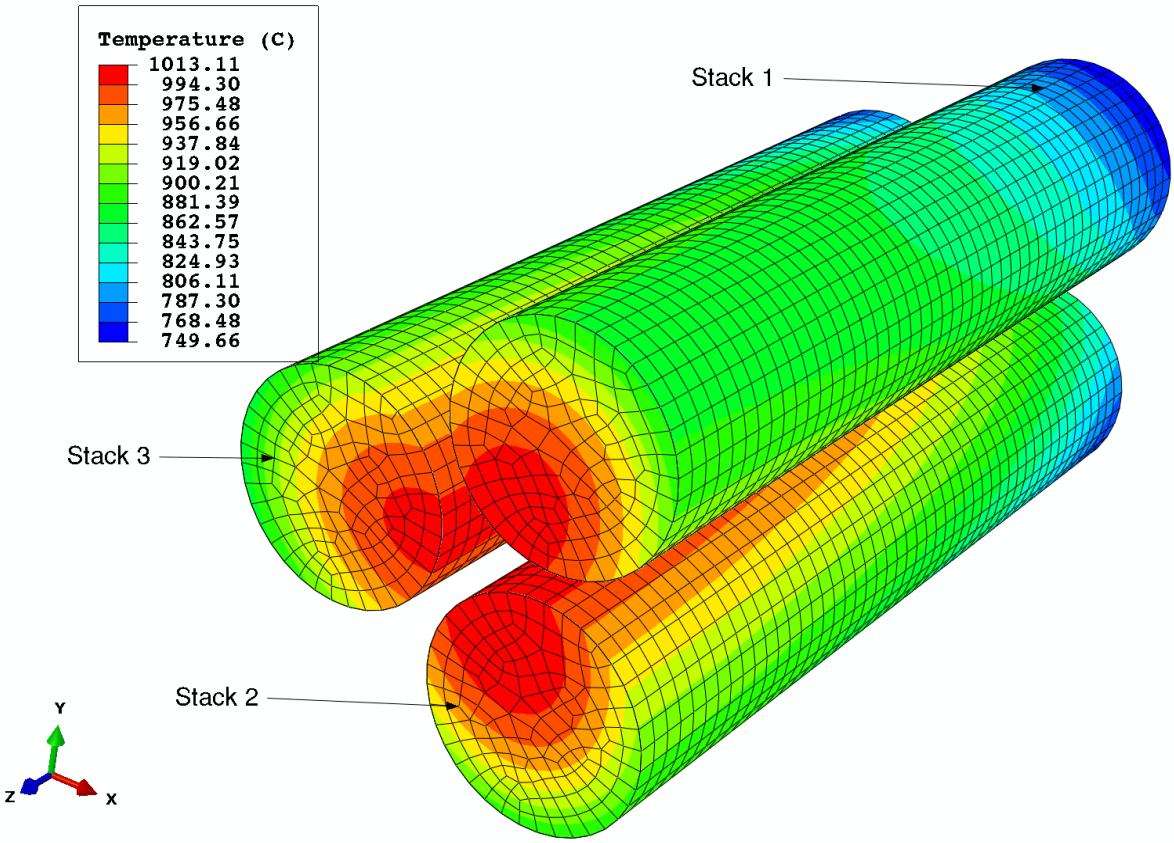

Figure 5. Temperature distribution in cutaway view of three fuel stacks of one AGR-2 capsule.

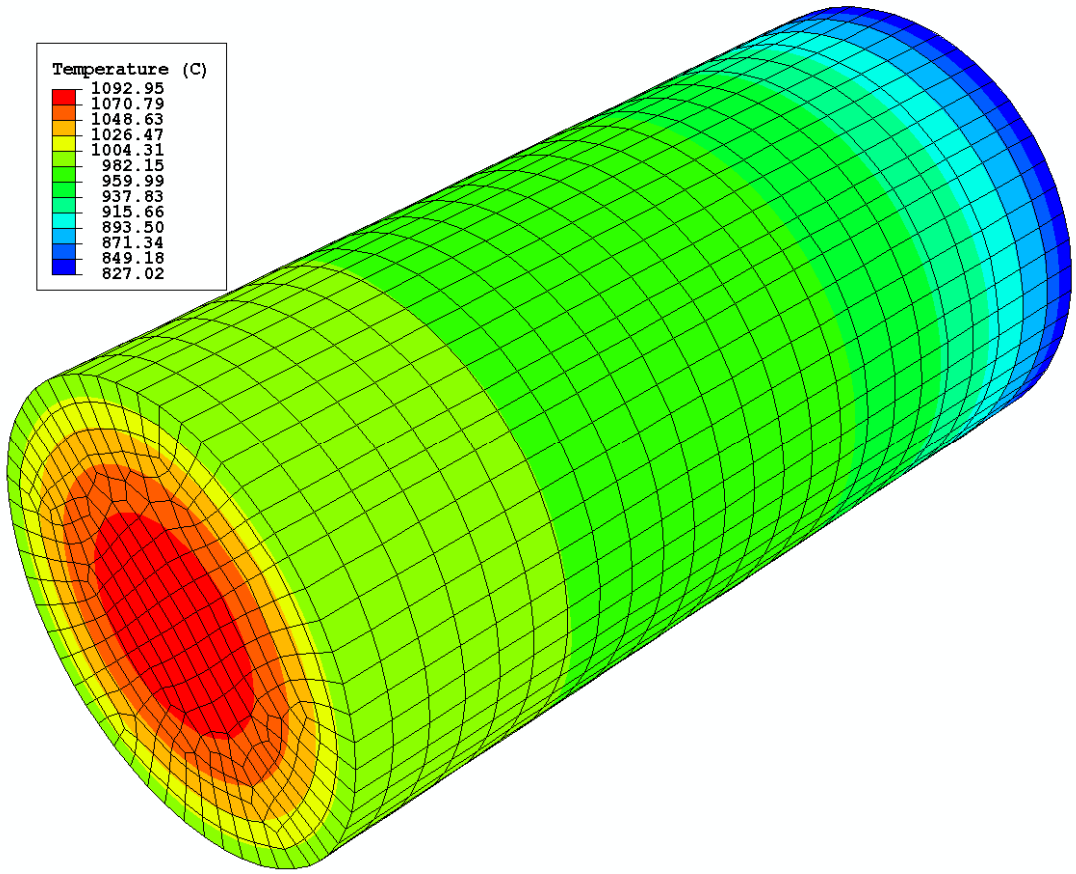

Figure 6. Temperature distribution in cutaway view of a fuel stack of one AGR-3/4 capsule.

3. TRISTRUCTURAL ISOTROPIC FUEL IRRADIATIONS

A series of AGR irradiation tests is being conducted in ATR at Idaho National Laboratory in support of development and qualification of TRISO-coated low enriched uranium carbide/oxide (LEUCO) fuel used in HTGRs. The first United State irradiation of modern TRISO fuel, AGR-1, was completed in 2009. However, there were no in-pile particle failures detected during post-irradiation examination and heavy metal contamination was low. Consequently, AGR-1 R/B data were not included in this analysis. However, AGR-2 and AGR-3/4 irradiations completed in 2013 and 2014, respectively, can provide adequate data for this fission product data analysis.

The AGR-2 test train was located in the large B-12 position on the left of the ATR core (as shown in Figure 7). The AGR-2 irradiation can provide data for R/B per failed particle because a few exposed kernels existed in the UCO fuel that was irradiated based on the quality control data (Hunn 2010). The AGR-3/4 test train was located in the Northeast Flux Trap inside the ATR driver fuel elements (Figure 7), allowing faster irradiation time and better control of neutron flux. For AGR-3/4, particle failures in all capsules were expected because of use of DTF fuel particles, whose kernels are identical to the driver fuel kernels but the coatings are designed to fail during irradiation. There are 80 DTF fuel particles in each AGR-3/4 capsule, which are located along the vertical centerline of each of the fuel compacts. The number of actual fuel failures and time of occurrences in each capsule are determined by looking at the temporal profile of the gross gamma counts monitored separately for each of the 12 AGR-3/4 capsules.

In addition to R/B data from the AGR-2 and AGR-3/4 irradiations, this analysis includes a few historical irradiations of LEUCO TRISO fuel conducted in the 1980s for comparison. These historical tests had either DTF particles or in-pile failures from which R/B data on fission gas releases from UCO kernels could be obtained. The four key irradiations are: (1) HRB-17/18 (General Atomics 1987), (2) COMEDIE-BD1 (Richards 1994), (3) HFR-B1 (ORNL 1994), and (4) HRB 21 (DOE 1995).

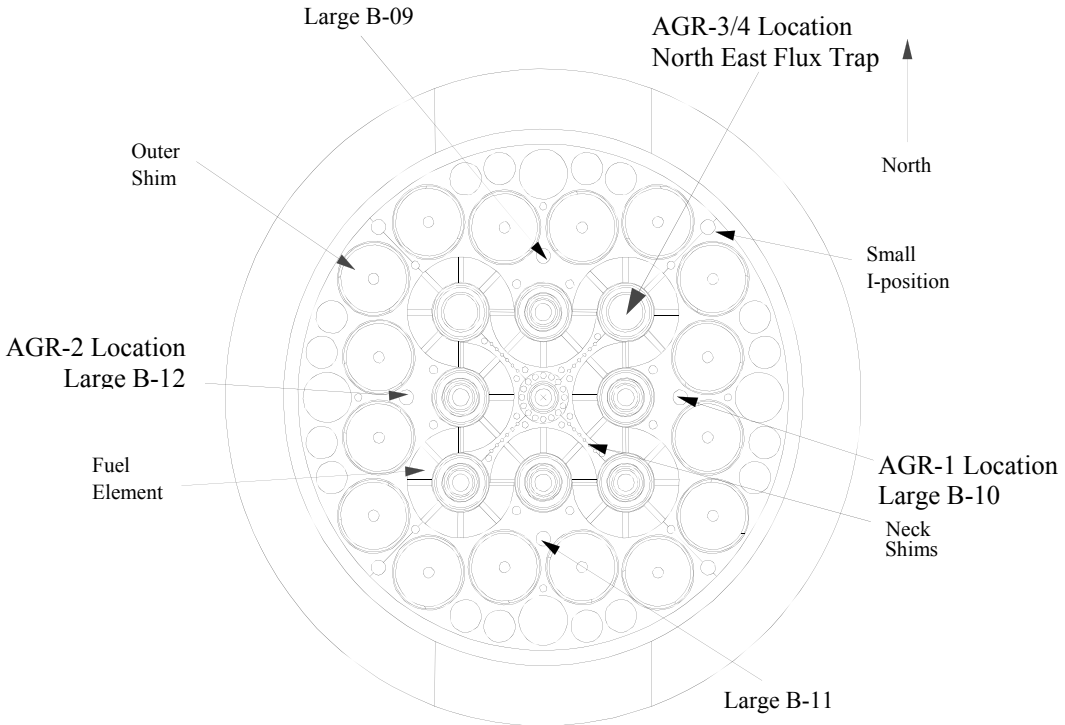

Figure 7. AGR-1, AGR-2, and AGR-3/4 locations in ATR core cross section.

3.1 Advanced Gas Reactor-2 Irradiation

AGR-2 is the second irradiation in a series of planned experiments to test the TRISO-coated low-enriched uranium fuel (Collin 2011a). This experiment is intended to demonstrate the performance of UCO and uranium dioxide (UO_2) fuel produced in a large (i.e., 15 cm/6-in.) coater. AGR-2 irradiation was completed in October 2013 after 559.2EFPDs. Figure 8 shows the sketch of a capsule in the AGR-2 irradiation test train. AGR-2 is comprised of six individual capsules, with approximately a 3.49-cm diameter and 15.24-cm long, stacked on top of each other to form the test train. A leadout tube holds the experiment in position and contains and protects the gas lines and TC wiring extending from the test train to the reactor penetration. Each AGR-2 capsule contains only one type of TRISO coated fuel particles. Each UCO capsule contains about 38,000 particles and each UO_2 capsule contains approximately 18,500 particles. United State UCO fuel particles are in Capsules 2, 5, and 6; United State UO_2 fuel particles are in Capsule 3; French UO_2 fuel particles are in Capsule 1; and South African UO_2 fuel particles are in Capsule 4. The French and South African capsule data are not presented or discussed in this report because of Cooperative Research and Development Agreement restrictions.

Even without DTF fuel particles included in capsules and no in-pile particle failure observed during irradiation, the AGR-2 irradiation still can provide R/B per failed particle data. This is due to exposed kernels in the test fuel that were irradiated. Quality control data (Collin 2011a) indicate that the 95% confidence defect fraction for an exposed kernel is 2.5E-05 for UCO fuel and 3.2E-5 for UO_2 fuel. Thus, on a statistical basis, there should be one exposed kernel in each UCO capsule and about one-half (or 50% chance) exposed kernel in each UO_2 capsule. Because exposed kernels should be a whole number, this potential particle failure in UO_2 capsules is inexplicable. Therefore, only R/B per failed particle data from three UCO capsules (i.e., 2, 5, and 6) are used in this analysis.

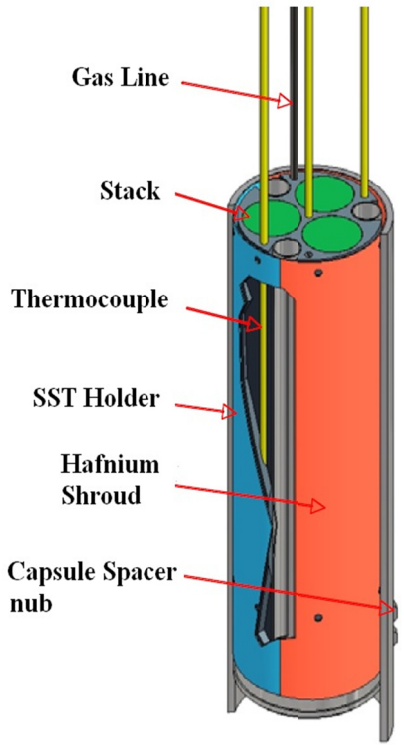

Figure 8. Sketch of an AGR-2 capsule.

3.1.1 Number of failed particles

Assuming no in-pile particle failures, fission gas release in an AGR-2 capsule comes from two main sources: exposed kernels and heavy metal contamination. The number of exposed kernels can be estimated from the defect fraction for exposed kernels in UCO fuel and the number of particles in each capsule. The heavy metal contamination fraction of fuel compacts is evaluated based on the fraction of free uranium from the UCO fuel batch, estimated from compacts that had no exposed kernels. Because fission gas released from heavy metal contamination also contributes to the measured release, this effect must be factored out to establish a true estimate of the release from exposed kernels.

Thus, the total measured R/B for a capsule without in-pile particle failure is a sum of releases from exposed kernels (first term) and heavy metal contamination (second term) as:

$$R_{Total} = R_p * f_{EK} * N + R_{HMC} * f_{HMC} * N \quad , \qquad (9)$$

Where: R_{Total} – Total R/B measured for a capsule

N – Total number of fuel particles in a capsule

R_{HMC} – R/B for release from heavy metal contamination, with amount of uranium equivalent to one kernel

f_{HMC} – Heavy metal contamination fraction from compacts without exposed kernels (g leached U/g U in compact)

R_p – R/B release from one exposed kernel (or R/B per failed particle)

f_{EK} – Exposed kernel fraction (g exposed U/g U in compact).

In addition, prior measurements at General Atomics (Martin 1993) have indicated that the release from finely dispersed heavy metal contamination is ten times that from an exposed dense kernel for the same amount of uranium ($R_{HMC} = 10R_p$). Using these results, Equation 9 can be derived as:

$$R_{Total} = N * R_p * (10 * f_{HMC} + f_{EK}) \qquad (10)$$

Subsequently, the total number of exposed kernels (N_{CF}) in one capsule can be expressed as the summation of number of exposed kernels and number of "equivalent" exposed kernels due to heavy metal contamination:

$$N_{CF} = N * (10 * f_{HMC} + f_{EK}) \qquad (11)$$

According to the AGR-2 fabrication quality assurance data taken from the AGR-2 test plan (Collin 2011a), the defect fraction for exposed kernels and heavy metal contamination fraction in each UCO capsule are $f_{HMC} = 3.9E-06$ and $f_{EK} = 2.5E-05$, respectively; and the total number of fuel particles in a capsule is $N = 38{,}000$. Additionally, no in-pile failures were observed during the AGR-2 irradiation, and detailed examination of the R/B data suggest that the increases observed in capsules 2, 5 and 6 are related to temperature increases. As a result, the final number of equivalent failed particles for each of the three AGR-2 UCO capsules can be calculated as:

$$N_{CF} = 3800 * (10 * 3.9 * 10^{-6} + 2.5 * 10^{-5}) \approx 2.5 \qquad (12)$$

3.1.2 Release-to-Birth Ratio per Failed Particle

As established in the previous section, the number of failed particles in one AGR-2 UCO capsule is estimated at 2.5, accounting for an exposed kernel and heavy metal contamination. Thus, the corresponding R/B per failed particle (R_p) can be calculated as:

$$R_p = R_{Total}/2.5 \quad . \qquad (13)$$

Detailed documentation of the FPMS measurement and processing methods for the AGR-2 FPMS data are contained in (Scates 2014a). This report also provides the basis for qualification of the FPMS data including R/B data for the entire AGR-2 irradiation. The temporal profiles of daily R/B per failed particle data for selected krypton isotopes are shown in Figure 9 and for xenon isotopes in Figure 10 for UCO Capsules 2, 5, and 6 during Cycles 148A and 148B. For the AGR-2 irradiation, only these release data are deemed suitable for this R/B data analysis. R/B data from the first cycle, 147A, were excluded to allow time for releases to reach their equilibrium state. Beyond Cycle 148B, no R/B data can be used because of relief valve issues during the next two cycles, 149A and 149B, and then cross-talk between capsules beginning in Cycle 150B (Scates 2014a). The cross-talk was probably caused by failure of the refractory gas lines in the experiment during experiment handling between ATR reactor cycles. Both relief valve issues and cross-talk failures allow the fission gas atoms from one capsule to get into the FPMS detector for another capsule. In these instances, R/B calculated using measurements from one detector are not necessarily representative of the release from the corresponding capsule; therefore, these R/Bs are not usable for this analysis.

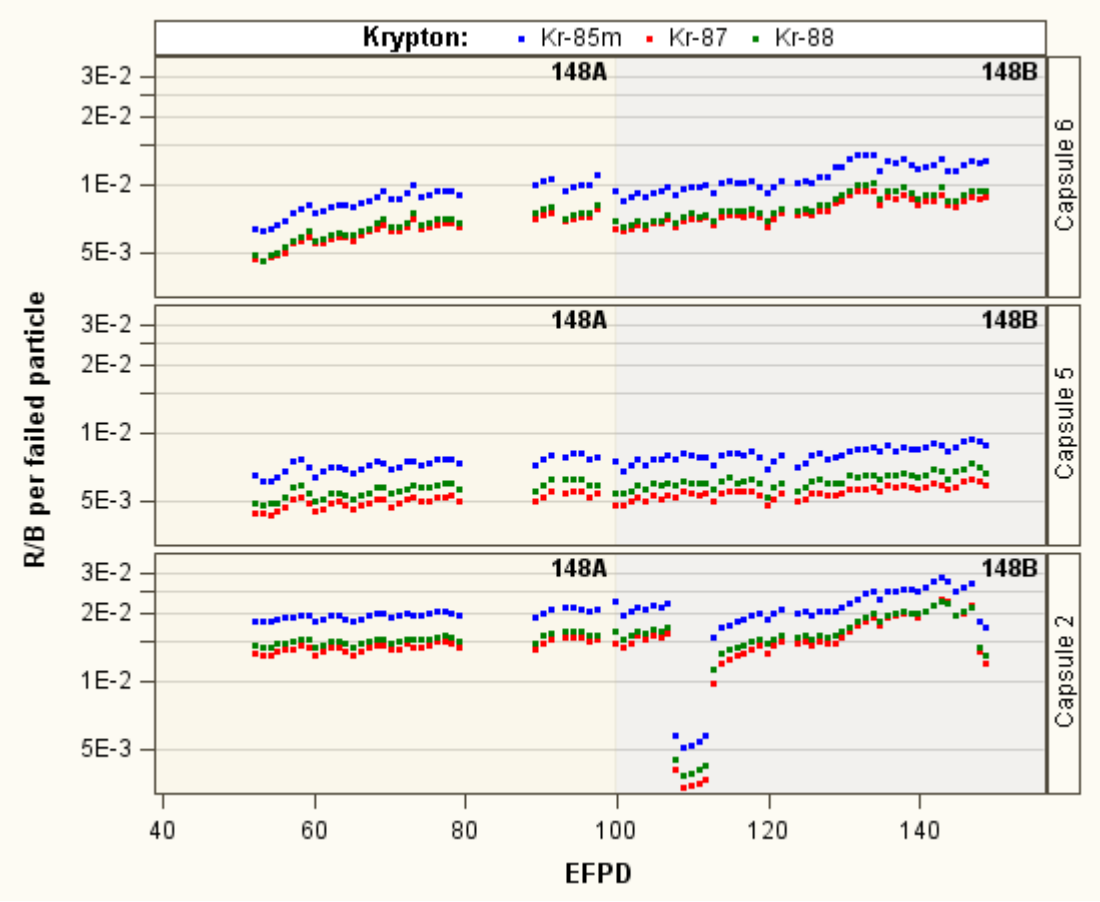

Figure 9. R/B per failed particle for krypton isotopes in AGR-2 UCO capsules.

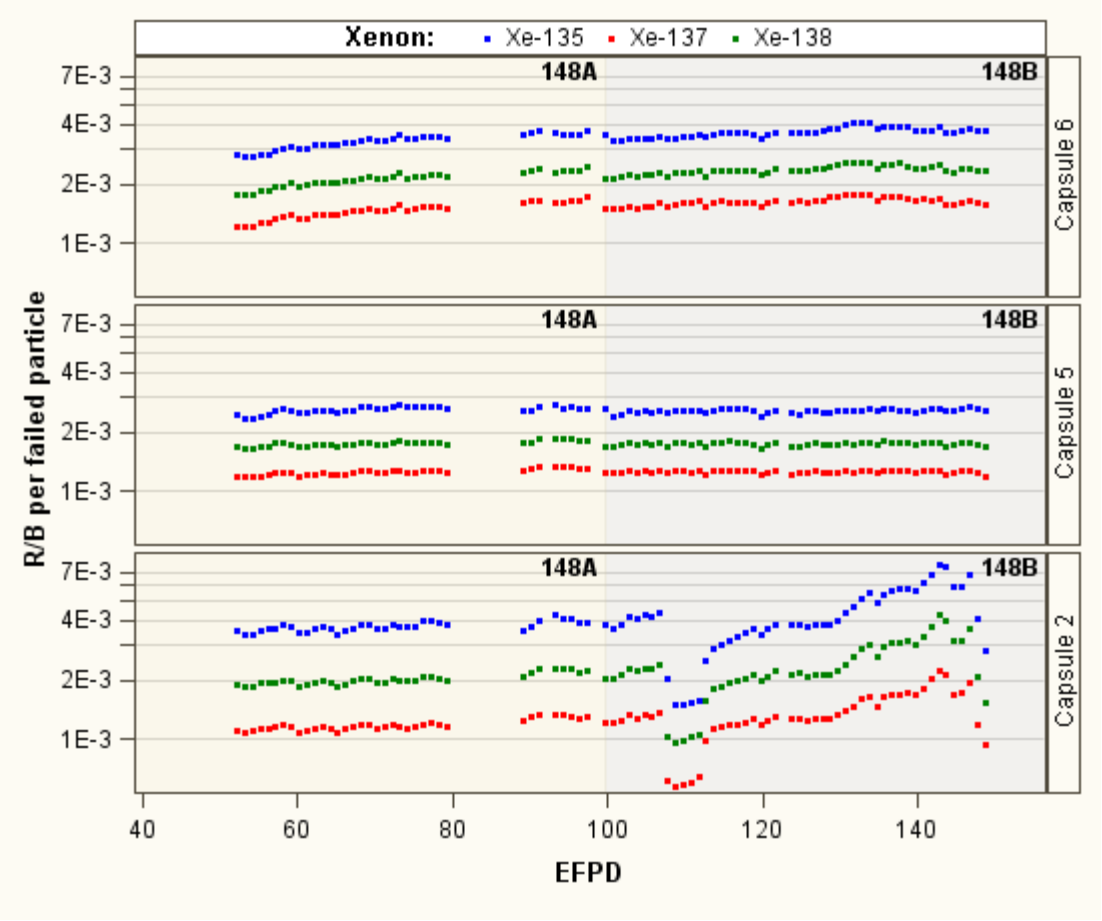

Figure 10. R/B per failed particle for xenon isotopes in AGR-2 UCO capsules.

In general, the R/B per failed particle data (Figure 9 and Figure 10) in all three capsules correlated well with averaged fuel temperatures (Figure 11) during both Cycles 148A and 148B; therefore, most of the data from these two cycles were used. For Capsules 5 and 6, R/B data and calculated fuel temperatures are fairly stable and correlate well with each other. For Capsule 2, a notable decrease of R/B was observed near the start of Cycle 148B for all six isotopes (bottom panels in Figure 9 and Figure 10). This corresponds well with a significant drop in fuel temperature (red dots in Figure 11) during that time when the capsule was put on all helium to deal with operational problems at ATR. Then, the R/B in Capsule 2 gradually increased for the rest of Cycle 148B in response to increasing fuel temperature (red dots in Figure 11). The broad range of Capsule 2 fuel temperatures between 1000 and 1400°C during Cycle 148B provides valuable data for establishing the correlation between R/B per failed particle and fuel temperature.

Table 2 presents a summary of AGR-2 R/B per failed particle data used for this regression analysis and for comparison with R/B from other TRISO fuel irradiation data. For krypton isotopes, the R/B per failed particle data are in the range of 0.30 to 2.87%. For xenon isotopes, R/B per failed particle data are in the lower ranges of 0.09 to 0.77%. It is apparent from Table 2 and the plots in Figure 9 and Figure 10 that the fission products of isotopes with lower decay constant (e.g., Kr-85m among krypton isotopes or Xe-135 among xenon isotopes) are consistently released at a higher rate for the entire time. Also, the temporal R/B plots for all isotopes are parallel with each other, indicating that R/B differences across isotopes are fairly constant despite changes in fuel temperatures. This fact demonstrates good consistency in the measurements of the FPMS.

Table 2. Summary of AGR-2 R/B data used in analysis for selected krypton and xenon isotopes.

Isotope	λ (s-1)	Number of Daily R/B Values	R/B per Failed Particle		
			Average	Minimum	Maximum
Kr-85M	4.30E-05	425	9.90E-03	3.72E-03	2.87E-02
Kr-87	1.52E-04	425	7.02E-03	3.00E-03	2.30E-02
Kr-88	6.78E-05	425	7.65E-03	3.08E-03	2.26E-02
Xe-135	2.12E-05	425	2.87E-03	1.50E-03	7.65E-03
Xe-137	3.01E-03	425	1.20E-03	5.24E-04	2.25E-03
Xe-138	8.19E-04	425	1.80E-03	8.98E-04	4.23E-03

3.1.3 Calculated Fuel Temperatures

A daily as-run thermal analysis was performed for the AGR-2 capsules using the commercial finite element heat transfer code ABAQUS (Hawkes 2014a). This thermal model was improved by incorporating gas gaps changing with irradiation time due to graphite shrinkage caused by neutron damage. The calculated volume average fuel temperature in each AGR-2 capsule is used for this analysis because the locations of failed particles are unknown. Figure 11 shows the calculated fuel temperature in three UCO capsules as a function of EFPDs for time periods when the R/B data were used in the analysis. A total of 255 daily volume-averaged fuel temperatures are used for the three UCO capsules, 2, 5, and 6.

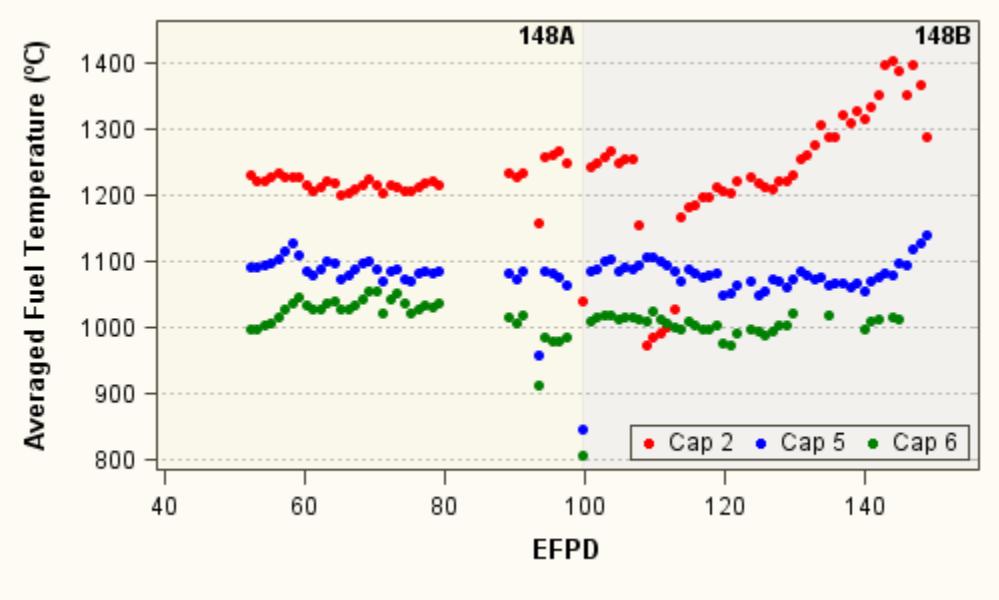

Figure 11. Volume-average fuel temperatures for AGR-2 UCO capsules.

3.2 Advanced Gas Reactor–3/4 Irradiation

AGR-3/4 is the third in this series of planned experiments to test TRISO coated LEU fuel. These were combined into a single experiment to reduce costs and overall program schedule. The primary objectives of the AGR-3/4 experiment are defined in PLN-3636, "Technical Program Plan for the Next Generation Nuclear Plant/Advanced Gas Reactor Fuel Development and Qualification Program." A detailed description of the experiment is provided in PLN-3867, "AGR-3/4 Irradiation Experiment Test Plan." The fuel to be irradiated in each AGR-3/4 capsule contains conventional TRISO driver fuel particles and DTF fuel particles. The UCO kernels of conventional fuel particles are similar to the baseline fuel used in the AGR-1 experiment. The DTF fuel particles contain kernels identical to the driver fuel kernels but their coatings are designed to fail under irradiation, leaving fission products to migrate through the surrounding materials (PLN-3867). The same number of DTF fuel particles was embedded along the vertical centerline in each compact to offer data on fission product diffusivity in fuel kernels and sorptivity and diffusivity in compact matrix and graphite materials. They are crucial data to support the refinement of fission product transport models and to assess the effects of sweep gas impurities on fuel performance and fission product transport (Collin 2011b). Therefore, AGR-3/4 gaseous fission product release data are the main focus of this analysis.

AGR-3/4 is comprised of 12 independently controlled and monitored capsules stacked on top of each other to form the test train using the full 1.22-m active core height (Figure 12). Each capsule contains four 3.81-cm long compacts, which were divided into eight nodes in the depletion analysis model (as shown by the far left column of Figure 12 for Capsule 6). Each fuel compact contains about 1,872 conventional UCO driver fuel coated particles and 20 DTF UCO fuel particles. A leadout tube holds the experiment in position and contains and protects the gas lines and TC wiring extending from the test train to the reactor penetration. Three TCs are located in Capsules 5, 10, and 12 and two TCs are in the remaining capsules. In order to assess the effects of sweep gas impurities on fuel performance and subsequent fission product transport, an impure gas was injected into Capsule 11 using additional flow controllers. This impure gas consists of 98% or 99% helium contaminated with CO, H_2O, and H_2, which are typically found in the primary circuit of HTGRs. Thus, each capsule would have combined helium/neon flow from a mass flow controller and an additional impure gas flow during the test sequence.

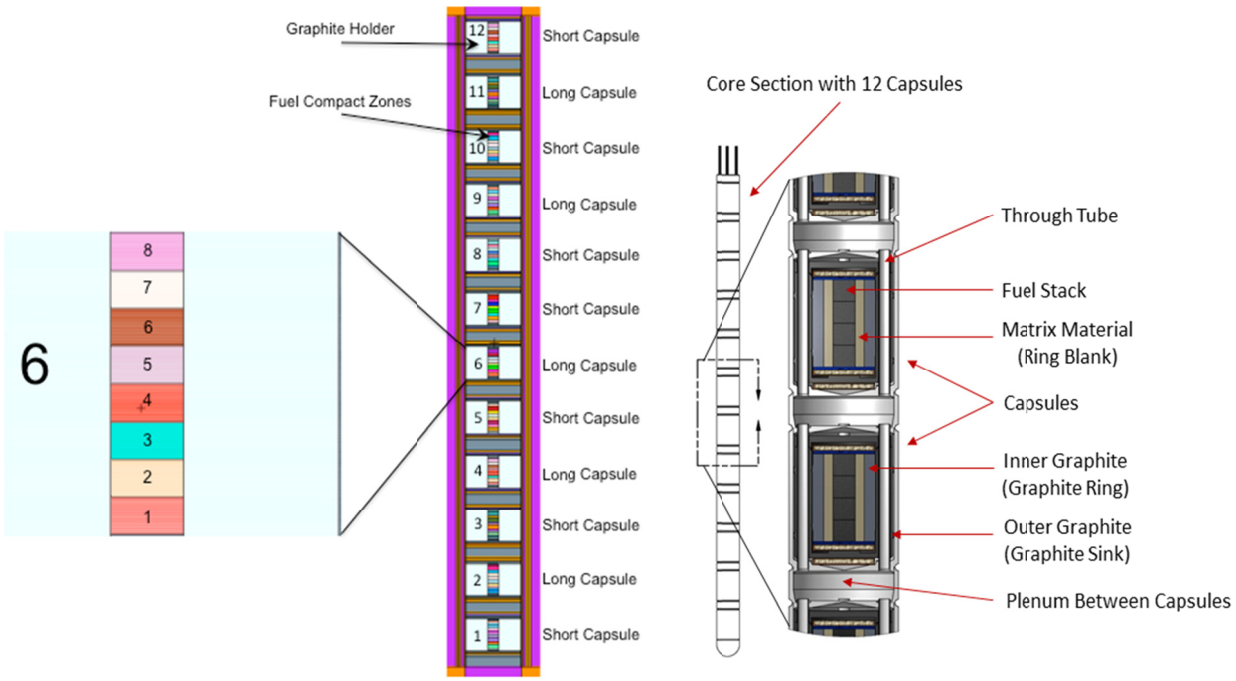

Figure 12. Axial (left) cross-section view and schematic (right) of AGR-3/4 capsules.

The irradiation was successfully completed in April 2014 after a total of 369.1 EFPDs. To accomplish the experiment objectives, the AGR-3/4 test train was inserted in the northeast flux trap location of the ATR core (as shown in Figure 7) during the outage portion of ATR Cycle 151A in December 2011. This ATR position allows achieving significant end-of-irradiation conditions in terms of peak burnup (15.3%) and maximum fast neutron fluence accumulation (5.3×10^{21} n/cm^2) for a larger amount of irradiated fuel contained in 12 capsules and for minimal irradiation time.

3.2.1 Number of Failed Particles

In each AGR-3/4 capsule, there were negligible numbers of exposed kernels and "equivalent" exposed kernels due to heavy metal contamination because AGR-3/4 fuel compacts have similar defect and contamination fractions, but the total number of fuel particles is much less than in an AGR-2 capsule (7,800 vs. 38,000). Also, based on AGR-1 irradiation results, it is reasonable to assume that there were no in-pile particle failures among the qualified driver fuel particles. Thus, the total number of fuel particle failures in each AGR-3/4 capsule is capped at a maximum of 80 failures.

The in-pile failures of DTF particles in a capsule are detected using the independent capsule-specific NaI(Tl) total radiation detector. Even though the detector is sensitive to each fuel particle failure, visually counting the exact number of failed particles during the AGR-3/4 irradiation was a challenging task due to multiple failures of DTF fuel particles occurring at the same time, partial failures, and high background activity of releases from already failed particles. Figure 13 shows two examples of multiple failure gross gamma spectra. The top plot shows an example of a "clean" multiple failure gross gamma spectra. This spectra output is from Capsule 7 and was collected on December 29, 2011, only 16 days after the start of AGR-3/4 irradiation when DTF particles began to fail. Each failure event is clearly defined by a rapid rise/fall activity, with a distinct increase in baseline count rate after each event. The area in the red oval and its blow-up plot on the top left represent one such instance where one failure occurred right after another. This double failure is further confirmed by the large step increase in baseline count rate after the event. During this 8-hour period five particle failures clearly occurred.

The bottom plot in Figure 13 shows an example of an "unclean" multiple failure gross gamma spectra. This spectra output is from Capsule 9 and was collected on December 10, 2013, near the end of AGR-3/4 irradiations (i.e., only one more cycle left), when all DTF particles in Capsule 9 were believed to have already failed. There are multiple "peaks" present in this output profile. However, as the baseline increases over time and more fuel has failed it becomes difficult to distinguish a failure from a "burp" (a small instantaneous release from a bubble of fission products). By closely reviewing the baseline of the 8-hour period here, it can be argued that there are between one and three failure events. Note that it is also possible that a partial failure occurred here or that a small pocket of trapped gas was released due to kernel microstructural changes with burnup at high temperature. In this case the uncertainty in particle failure count was high.

The challenges in the failure detection process could lead to high uncertainty of total number of particle failures in some capsules. Therefore, each inspection period provides three estimates of failure counts: (1) best-estimate, (2) maximum, and (3) minimum (as shown in Figure 15). For Capsule 1 (plots on the top of Figure 15) the three failure estimates are quite different from each other, indicating high counting uncertainty. By contrast, for Capsule 9 (plots on the bottom of Figure 15), the three failure estimates are very similar, indicating low counting uncertainty or high confidence about the number of particle failures. Table 3 presents some examples of weekly failure best estimates and Figure 16 plots the daily interpolated best-estimated failure counts as a function of EFPDs for 12 AGR-3/4 capsules. For most capsules, fuel failures occurred soon after the start of irradiation in the first cycle (i.e., first 55 EFPDs). For a few other capsules (e.g., Capsules 2 and 3), fuel failures occurred throughout irradiation. In three capsules (i.e., 2, 3, and 9), the final best estimated failure counts are higher than the number of DTFs and are capped at 80.

Table 3. Weekly cumulative estimated number of failed particles in AGR-3/4 capsules.

Date	14-Dec-11	21-Dec-11	28-Dec-11	4-Jan-12	11-Jan-12	18-Jan-12	25-Jan-12	2-Feb-12	8-Feb-12	3-May-12	15-Jan-13	7-Jul-13	10-Oct-13	11-Jan-14	9-Apr-14
Capsule					**151A**					**151B**	**152B**	**154A**	**154B**	**155A**	**155B**
12	0	1	1	1	1	6	23	35	40	40	40	40	40	40	40
11	0	0	0	2	10	18	25	44	57	66	66	67	69	69	69
10	0	0	5	9	19	44	47	47	47	47	47	47	47	47	47
9	0	1	19	33	56	78	79	79	79	79	83	83	85	90	90
8	0	0	25	35	52	66	66	66	66	66	67	67	68	73	78
7	0	0	31	34	37	39	39	42	42	43	50	52	52	52	52
6	0	2	13	30	43	44	44	44	44	45	45	45	45	46	47
5	0	0	8	16	33	40	40	40	40	40	40	40	45	47	54
4	0	1	11	27	45	58	58	58	58	62	71	71	71	71	76
3	0	0	7	13	13	21	27	29	29	54	71	72	94	96	96
2	0	0	0	7	17	24	32	45	50	51	60	66	82	86	91
1	0	0	0	1	2	8	20	25	30	39	39	39	39	39	41

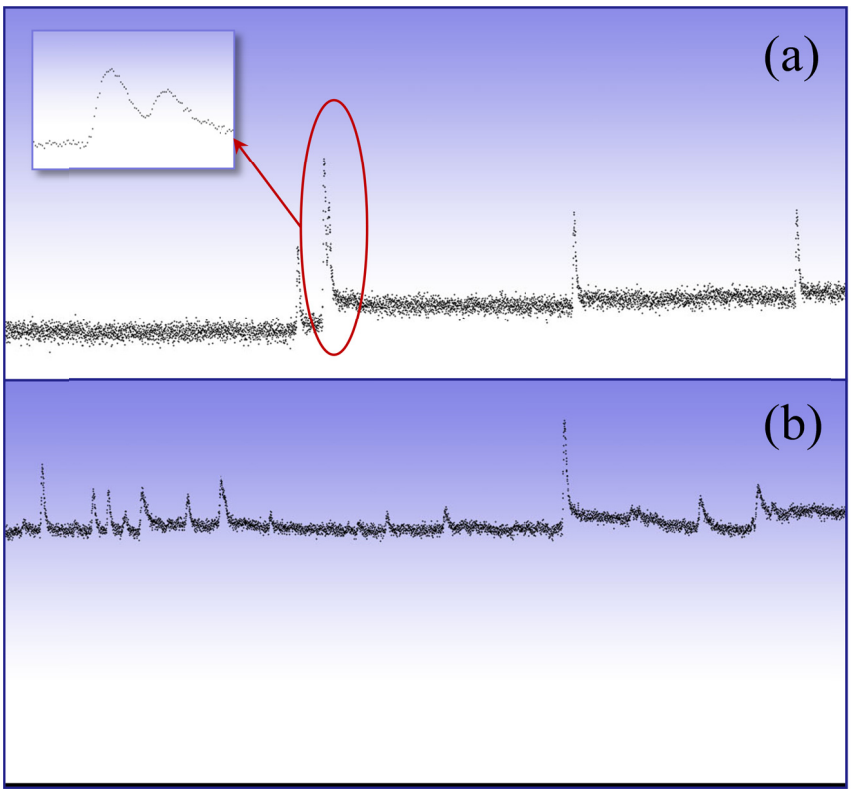

Figure 13. Examples of multiple failure gross gamma spectra: (a) – “clean” multiple failure and (b) – “unclean” multiple failure.

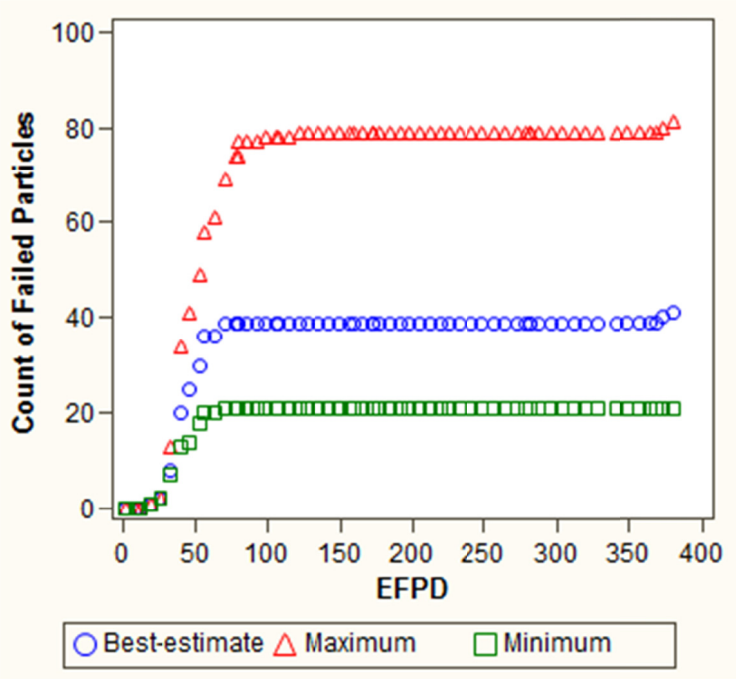

Figure 14. High uncertainty of particle failure count in Capsule 1.

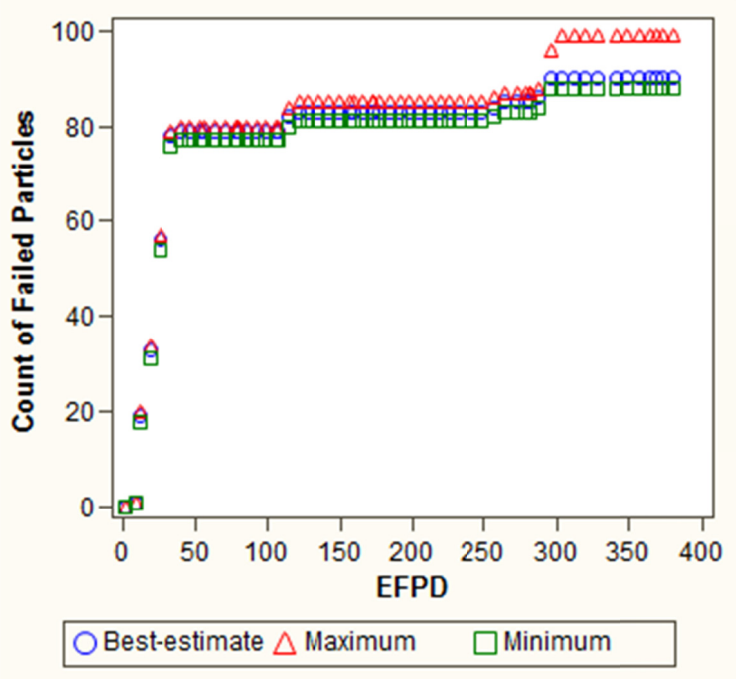

Figure 15. Low uncertainty of particle failure count in Capsule 9.

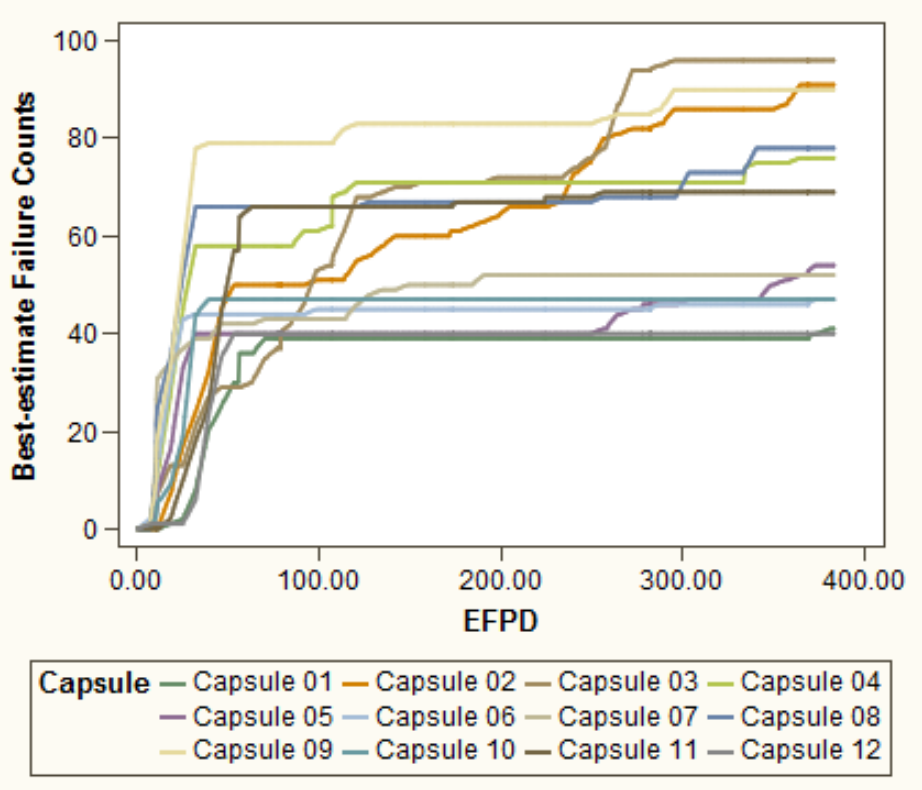

Figure 16. AGR-3/4 best-estimate failure counts.

3.2.2 Release-to-Birth Ratio per Failed Particle

The qualification status of AGR-3/4 R/B data was reported in (Scates 2014b). As stated in the previous section, it is essential that equilibrium is achieved for the measured release rates at the downstream detector to reflect the true release rate in the capsule. Thus, only R/B data during fission product release equilibrium are used for this analysis. The R/B data excluded from regression analysis are: (1) the first cycle, (2) the first 10 days after each reactor startup following a long cycle outage, and (3) the first 3 days after reactor restart following a short scram. During the first cycle, Cycle 151A, about 60% of all DTF fuel particles failed by the cycle end. The uncertainty of daily failed particle counts is large because failure counts were made on a weekly basis. In addition, equilibrium may not have been achieved due to multiple particle failures throughout the cycle and rapid changes of material thermal properties due to fast fluence exposure. This causes large variation of R/B per failed particle during the first cycle in all capsules. At the same time, the calculated peak fuel temperatures are fairly constant. Consequently, R/B data during the first cycle are excluded from analysis. In order to avoid higher than normal fission product releases after each reactor outage due to their accumulation at much lower temperature, the first 10 days after long outages between reactor cycles are excluded and the first 3 days after short outages within a reactor cycle are excluded. Additionally, R/B data with uncertainty greater than 50% and R/B data acquired for too short intervals (20-minute instead of 8-hour interval) are also excluded. After these exclusions, the uncertainties of suitable R/B data for selected krypton and xenon isotopes are around 6% (as presented in Table 1). In spite of this R/B data filtering, there remain more than enough data for use in this analysis (as shown by Column 3 in Table 4).

Table 4. Summary of AGR-3/4 R/B data used in analysis for selected krypton and xenon isotopes.

Isotope	Decay Constant λ (s-1)	N# of Daily R/B Values	R/B per Failed Particle		
			Average	Minimum	Maximum
Kr-85M	4.30E-05	3,084	2.0E-02	2.1E-03	7.3E-02
Kr-87	1.52E-04	3,079	1.3E-02	1.3E-03	6.0E-02
Kr-88	6.78E-05	3,066	1.6E-02	1.6E-03	6.5E-02
Xe-135	2.12E-05	3,079	8.5E-03	6.7E-04	3.6E-02
Xe-137	3.01E-03	3,079	1.9E-03	1.5E-04	1.2E-02
Xe-138	8.19E-04	3,079	4.1E-03	2.8E-04	2.3E-02

Figure 17 and Figure 18 show daily averaged R/B per failed particle data for three krypton isotopes: Kr-85m, Kr-87, and Kr-88 obtained in Capsules 1 through 12 as a function of EFPDs throughout AGR-3/4 irradiation. Figure 19 and Figure 20 show daily averaged R/B per failed particle for three xenon isotopes: Xe-135, Xe-137, and Xe-138. These are the daily R/B data used for this fission product data analysis. Table 4 shows the average, minimum, and maximum values of R/B per failed particle for six selected isotopes. The krypton R/B per failed particle data vary widely in the range of 0.13 to 7.3% and the xenon R/B per failed particle is somewhat lower and in the range of 0.015 to 3.6%. The R/B data for AGR-3/4 irradiation also follow the same pattern as for AGR-2 in that the fission products of isotopes with lower decay constants (e.g., Kr-85m among krypton isotopes or Xe-135 among xenon isotopes) are consistently released at a higher rate for the entire time relative to isotopes with a higher decay constant. This indicates the impact of decay constants on fission product releases. Also, the temporal R/B plots for all isotopes are parallel with each other, indicating that R/B differences across isotopes are fairly constant despite changes in fuel temperatures. This fact demonstrates good consistency in the measurements of the FPMS.

The R/B per failed particle correlation with peak fuel temperature is observable when comparing R/B temporal plots in Figure 17 through Figure 20 and fuel temperature plots in Figure 21. Especially during the last cycle, Cycle 155B, the R/B per failed particle increased in response to a notable increase in peak fuel temperatures in most capsules.

3.2.3 Calculated Fuel Temperatures

A daily as-run thermal analysis was also performed for AGR-3/4 capsules using the commercial finite element heat transfer code ABAQUS (Hawkes 2014b). As for AGR-2 capsules, this thermal model incorporates the gas gaps changing with irradiation time due to graphite shrinkage caused by neutron damage. The model of gas gap change was rigorously calibrated to achieve the best fit between predicted temperatures at TC locations and TC readings over the entire irradiation. Contrary to AGR-2, the calculated peak fuel temperature in each AGR-3/4 capsule is used for R/B data analysis, because the DTF fuel particles are located along the axial centerline of fuel compacts, which are exposed to the highest temperature in each capsule as shown in Figure 6.

There are three distinct groups of peak fuel temperatures among the 12 AGR-3/4 capsules. Figure 21 shows daily-averaged calculated peak fuel temperatures in 12 capsules as a function of EFPDs for the entire irradiation (filtered data not used in the analysis are not included). The calculated peak fuel temperatures range broadly from 850°C (lowest temperature in Capsule 12 as shown by blue dots in the top frame of Figure 21) to 1400°C (highest temperature in Capsule 7 as shown by red dots in the bottom frame of Figure 21). This wide fuel temperature range provides adequate data to establish the relationship between R/B per failed particle and temperature.

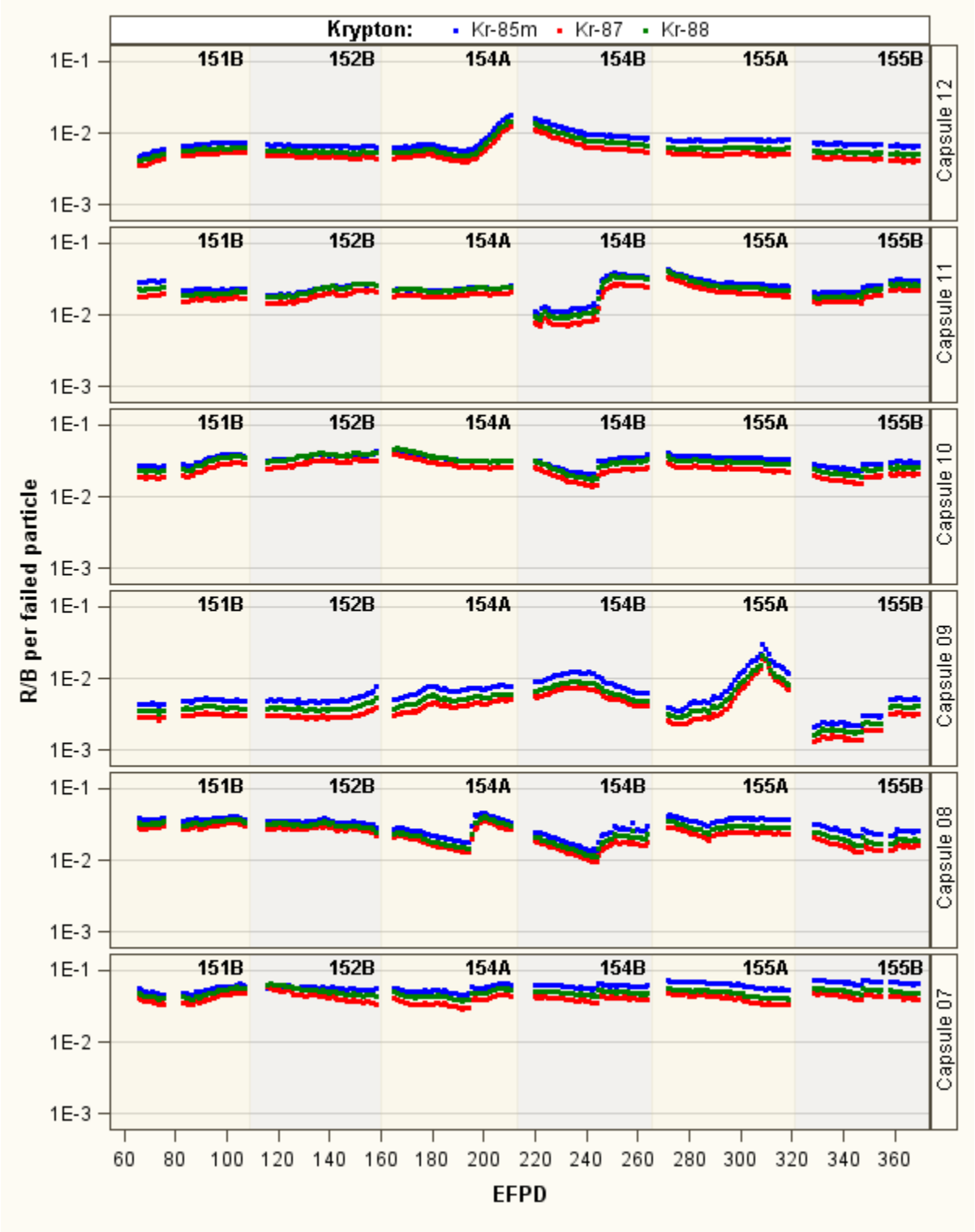

Figure 17. R/B per failed particle for krypton isotopes in AGR-3/4 Capsules 7 through 12.

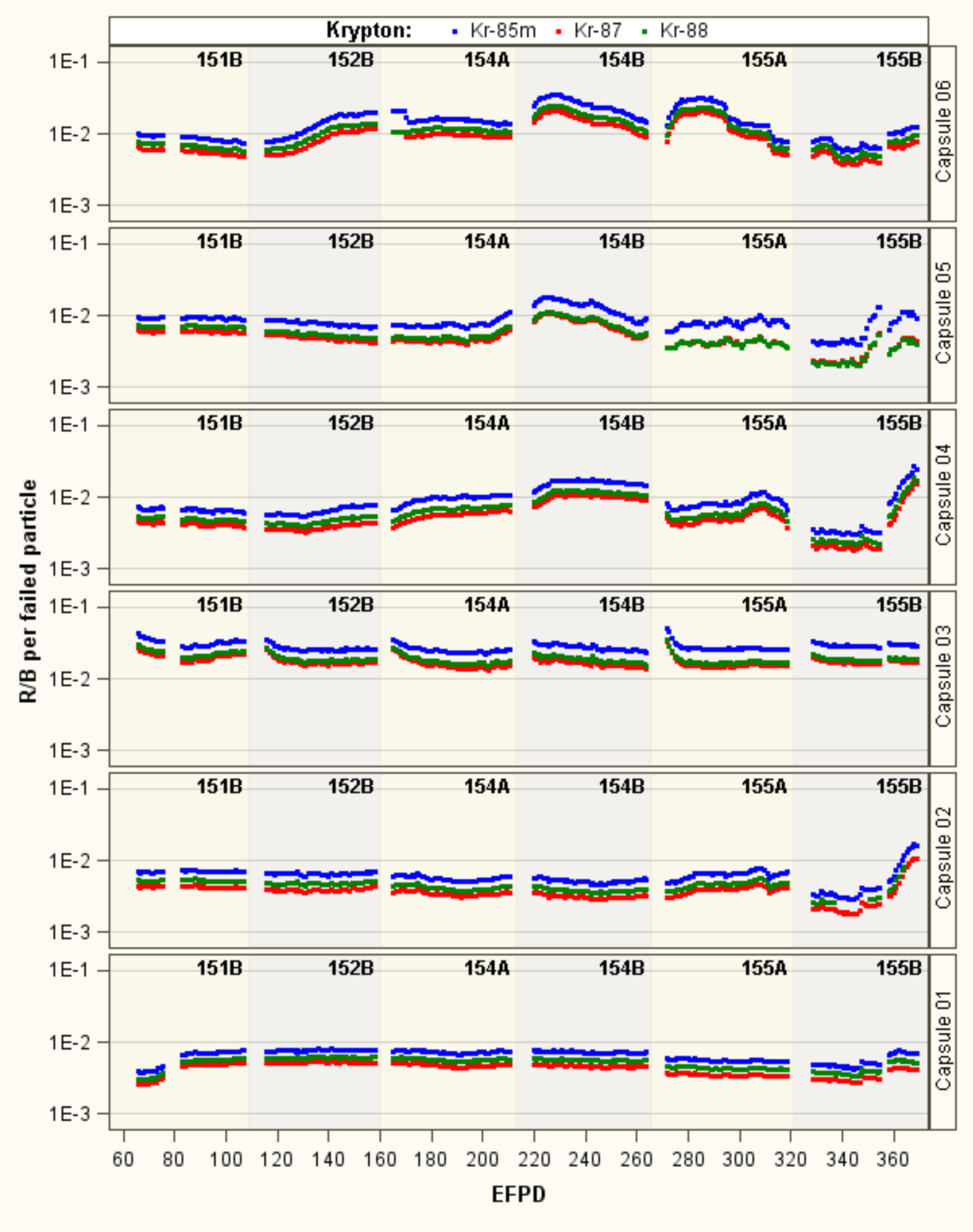

Figure 18. R/B per failed particle for krypton isotopes in AGR-3/4 Capsules 1 through 6.

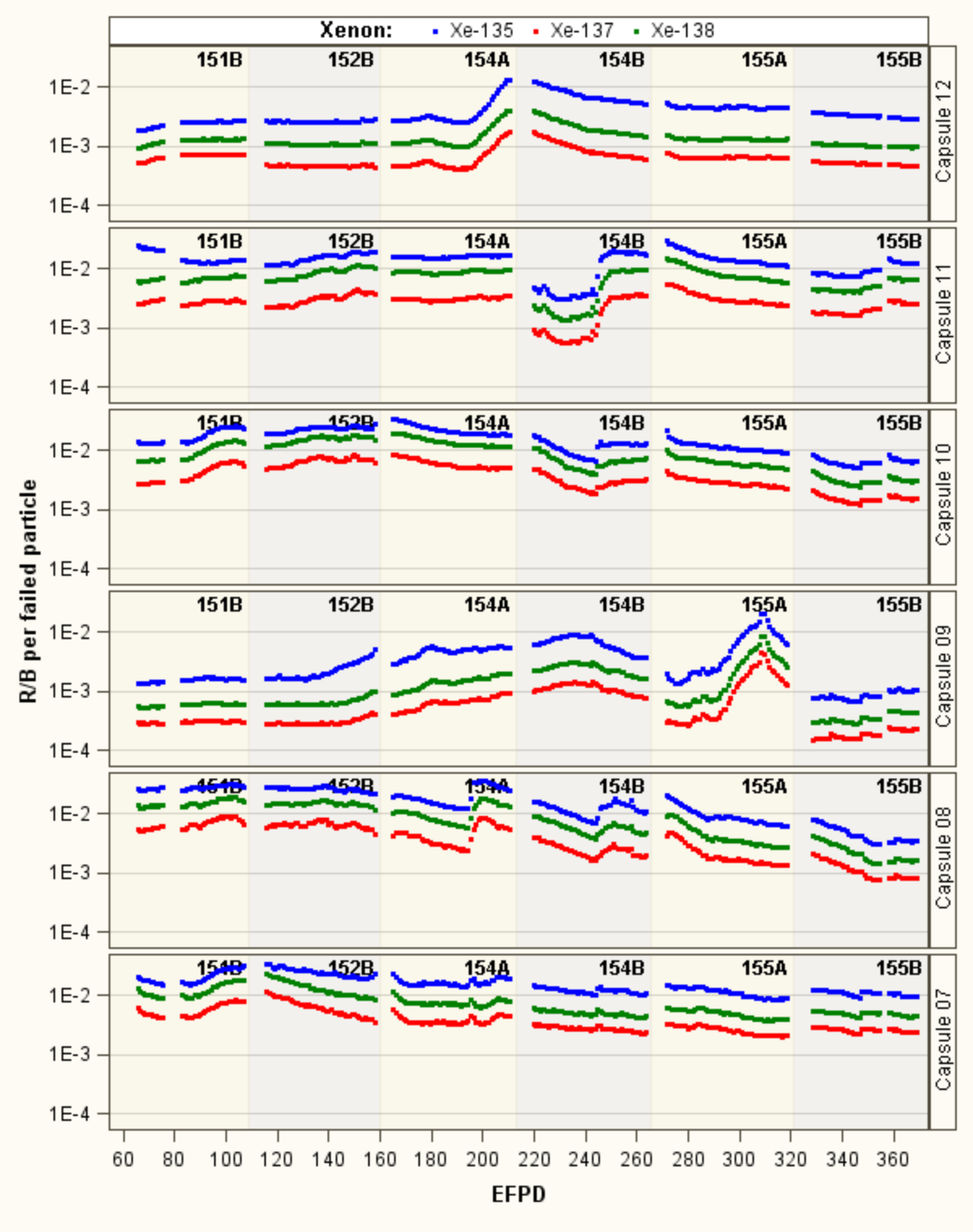

Figure 19. R/B per failed particle for xenon isotopes in AGR-3/4 Capsules 7 through 12.

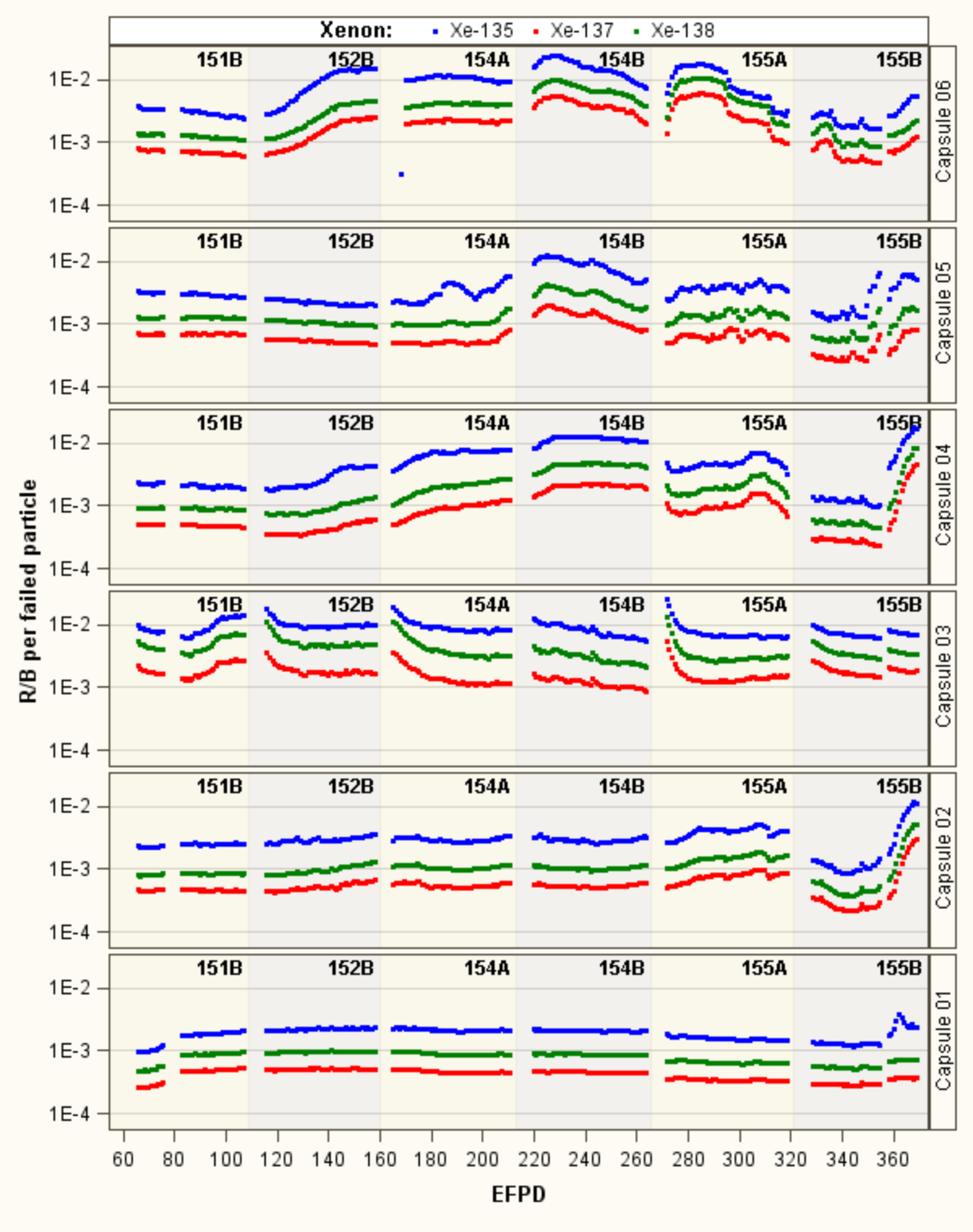

Figure 20. R/B per failed particle for xenon isotopes in AGR-3/4 Capsules 1 through 6.

.

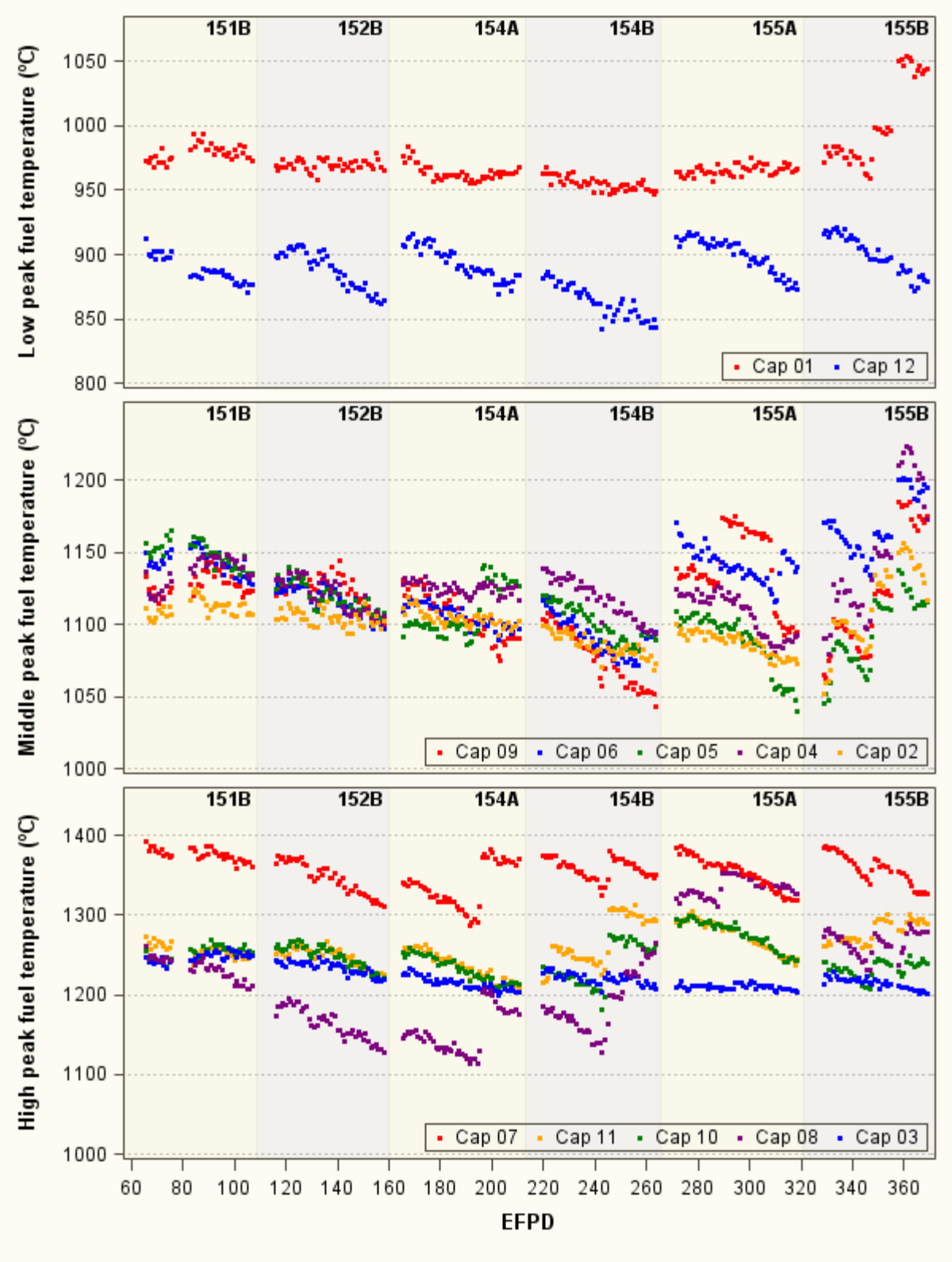

Figure 21. Peak fuel temperatures for AGR-3/4 Capsules.

3.3 Historical Irradiations

There are a few historical irradiations of low enriched UCO TRISO fuel that had either DTF particles or had in-pile failures that can provide additional R/B data for comparison to the AGR-3/4 and AGR-2 data. In many cases, these experiments were moisture injection experiments to study hydrolysis effects on fission gas release from UCO kernels, but the R/B prior to moisture injection provides valuable data for comparison here. Table 5 summarizes the R/B per failed particle data for Kr-85m from four key irradiations: (1) HRB-17/18 (General Atomics 1987), (2) COMEDIE-BD1 (Richards 1994), (3) HFR-B1 (ORNL/TM-12740), and (4) HRB-21 (DOE-HTGR-100229). Results are plotted using the average fuel temperature unless noted otherwise.

Table 5. R/B per failed particle for Kr-85m from four key historic irradiations.

Experiment	Fuel Temperature (°C)	R/B per Failed Particle
HRB-17 and18[a]	840	4.0E-4
COMEDIE	1160	1.0E-2
HFR-B1 Capsule B[b]	1140	8.0E-3
	1015	3.0E-3
	912	2.0E-3
HRB-21[c]	950 (max) / 932	9.0E-3
		7.0E-3

a. Results were identical for two independent capsules run at the same time in different locations in the reactor (General Atomics 1987).
b. 125 °C added to TC temperatures to get fuel temperatures as recommended in report (see Table 6.4.33 in ORNL/TM-12740).
c. First R/B value represents value for first particle failure (assumed to be at the maximum temperature) and second value is an average based on the total number of estimated failures (DOE-HTGR-100229).

Table 6 presents the R/B per failed particle for several krypton and xenon isotopes for one irradiation condition extracted from the COMEDIE test results used to compare its n values (or slope between R/B and reciprocal decay constant in natural logarithm scale) to AGR results.

Table 6. COMEDIE R/B data for krypton and xenon isotopes

Isotope	Half-life (min.)	R/B per failed particle
Kr-89	3	2.30E-03
Kr-87	73	7.10E-03
Kr-88	180	8.40E-03
Kr-85m	250	1.10E-02
Xe-137	3.8	8.10E-04
Xe-138	13	1.20E-03
Xe-133m	3,200	2.90E-02
Xe-133	7,200	8.00E-02

4. ANALYSIS RESULTS AND DISCUSSION

4.1 Release-to-Birth Ratio Correlation with Decay Constants

As specified in Section 2.1.4, the n values for TRISO coated fuel particles can range between 0.1 and 0.5, depending on the recoil effect of the particle coatings. For a constant fuel temperature, Equation 7 can be rewritten as:

$$\ln R_p = n \ln \frac{1}{\lambda} + C' \quad , \quad (14)$$

Where C' is a new constant including the reciprocal fuel temperature term. In order to study the correlation between fission product releases and decay constants, a few sets of R/B per failed particle data for selected krypton and xenon isotopes were taken for 2 days: one representing low burnup for a day near the start of irradiation (second cycle, Cycle 151B) and one representing high burnup (up to 15%) for a day near the end of irradiation (last cycle, Cycle 155B). For each capsule, assuming the fuel temperature is constant during a day, the n value can be estimated as the slope between $\ln R_p$ and $\ln \frac{1}{\lambda}$ for isotopes of each gas element (i.e., krypton or xenon). Because peak fuel temperatures are quite different across AGR-3/4 capsules, these sets of R/B can help reveal the impact of fuel temperature and burnup on n values. Figure 22 illustrates the slopes for three fuel temperatures (see legends) and two burnup levels (Cycles 151B and 155B) for krypton and xenon elements. This figure also includes a data set in the COMEDIE test presented in Table 6 (purple stars). It is apparent that all fitted lines are quite parallel for both krypton and xenon isotopes, indicating that temperature and burnup have no significant influence on n values. Also, the slopes of AGR-3/4 R/B data are similar to the slope of the COMEDIE R/B data.

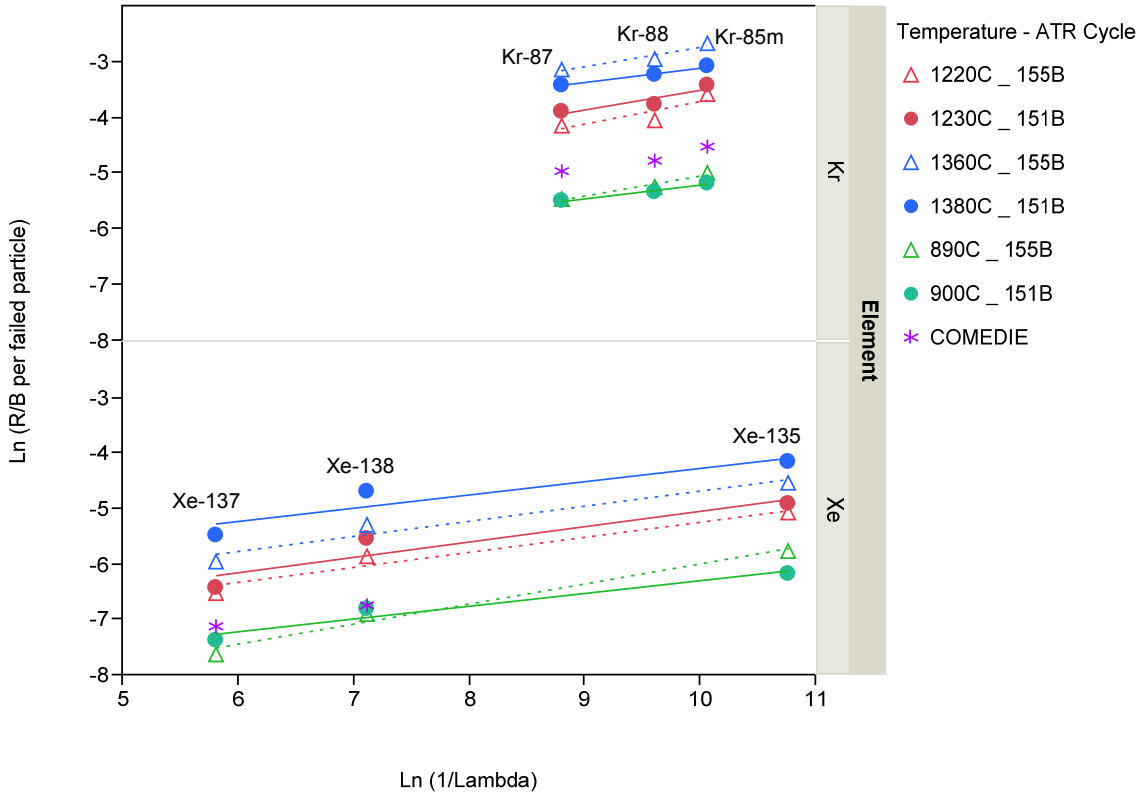

Figure 22. Slopes between ln R/B per failed particle and ln 1/λ for different temperatures and burnup.

Figure 23 and Figure 24 show daily *n* values for krypton and xenon isotopes for the twelve AGR-3/4 capsules as a function of EFPDs. Figure 25 shows daily *n* values for the three AGR-2 capsules (2, 5, and 6) during ATR Cycles 148A and 148B. In general, *n* values for krypton isotopes (blue dots) and for xenon isotopes (red dots) are comparable and on average equal to about 0.3. For AGR-3/4, except for the first cycle, the *n* values are fairly constant over the entire irradiation, indicating no significant burnup influence on fission product release, when the peak burnup reached as high as 15.3 % fissions per initial metal atom. Similar behavior of *n* values is also observed for AGR-2 irradiation (Figure 25).

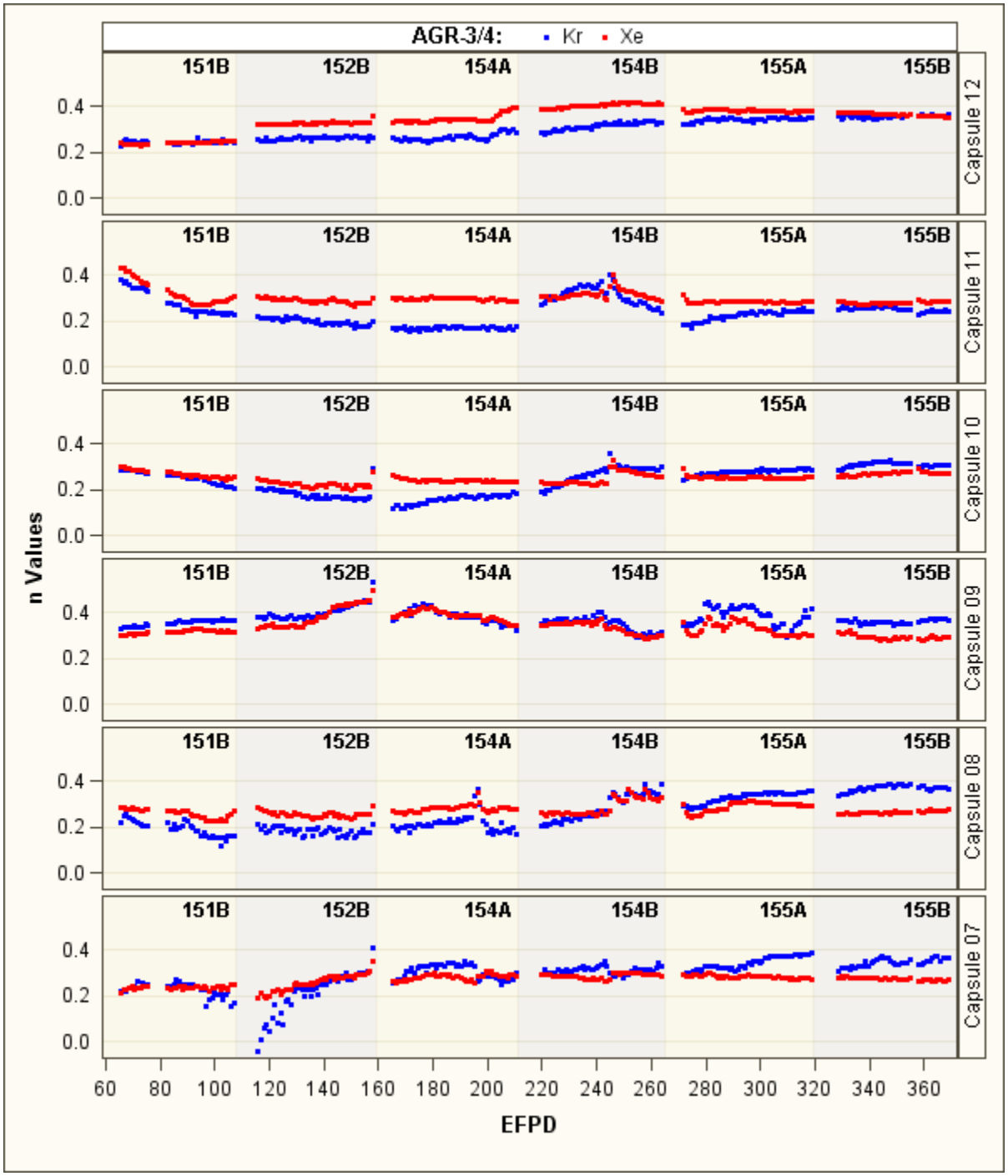

Figure 23. Krypton and xenon *n* values as function of EFPD for AGR-3/4 Capsules 7 through 12.

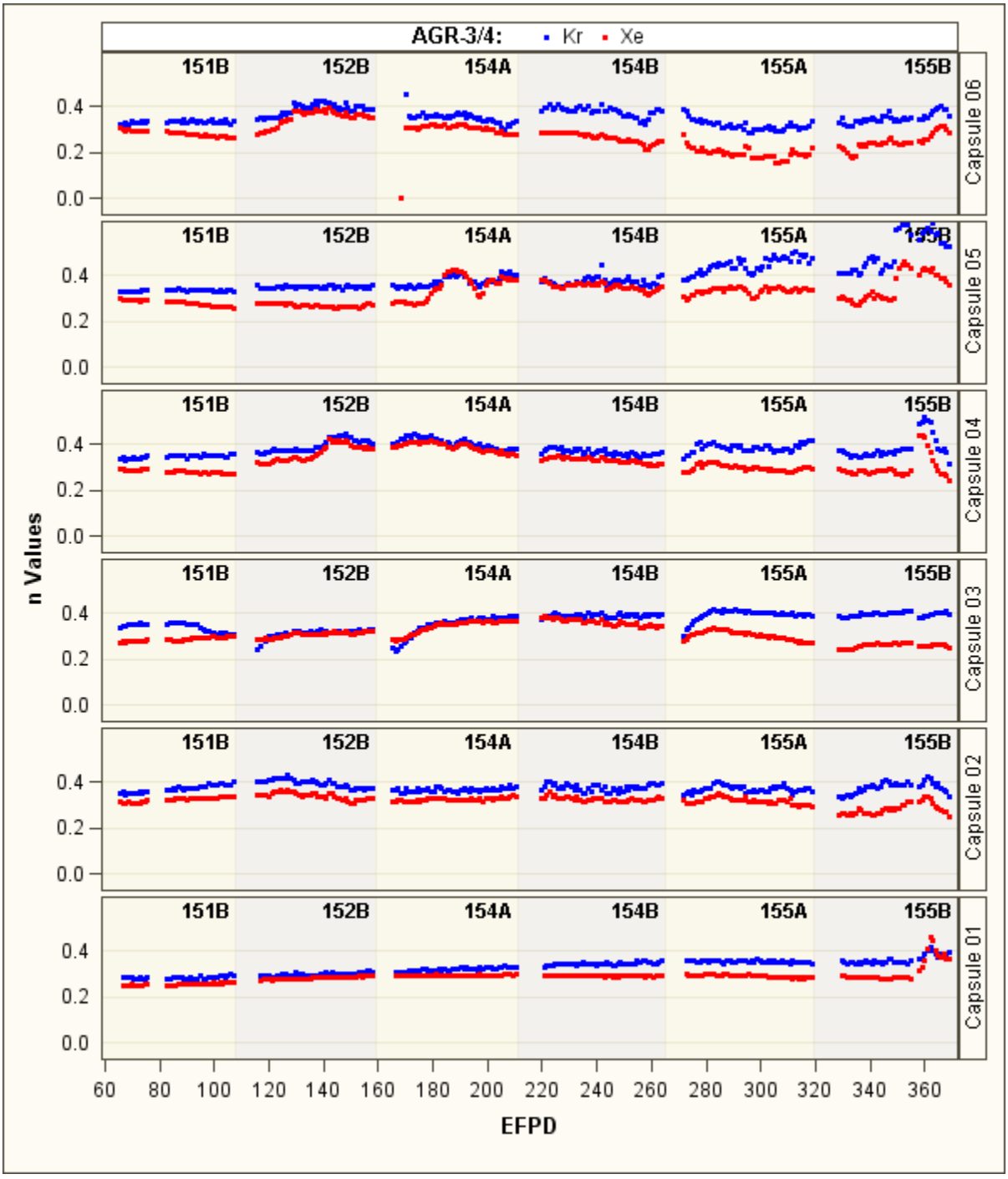

Figure 24. Krypton and xenon *n* values as function of EFPD for AGR-3/4 Capsules 1 through 6.

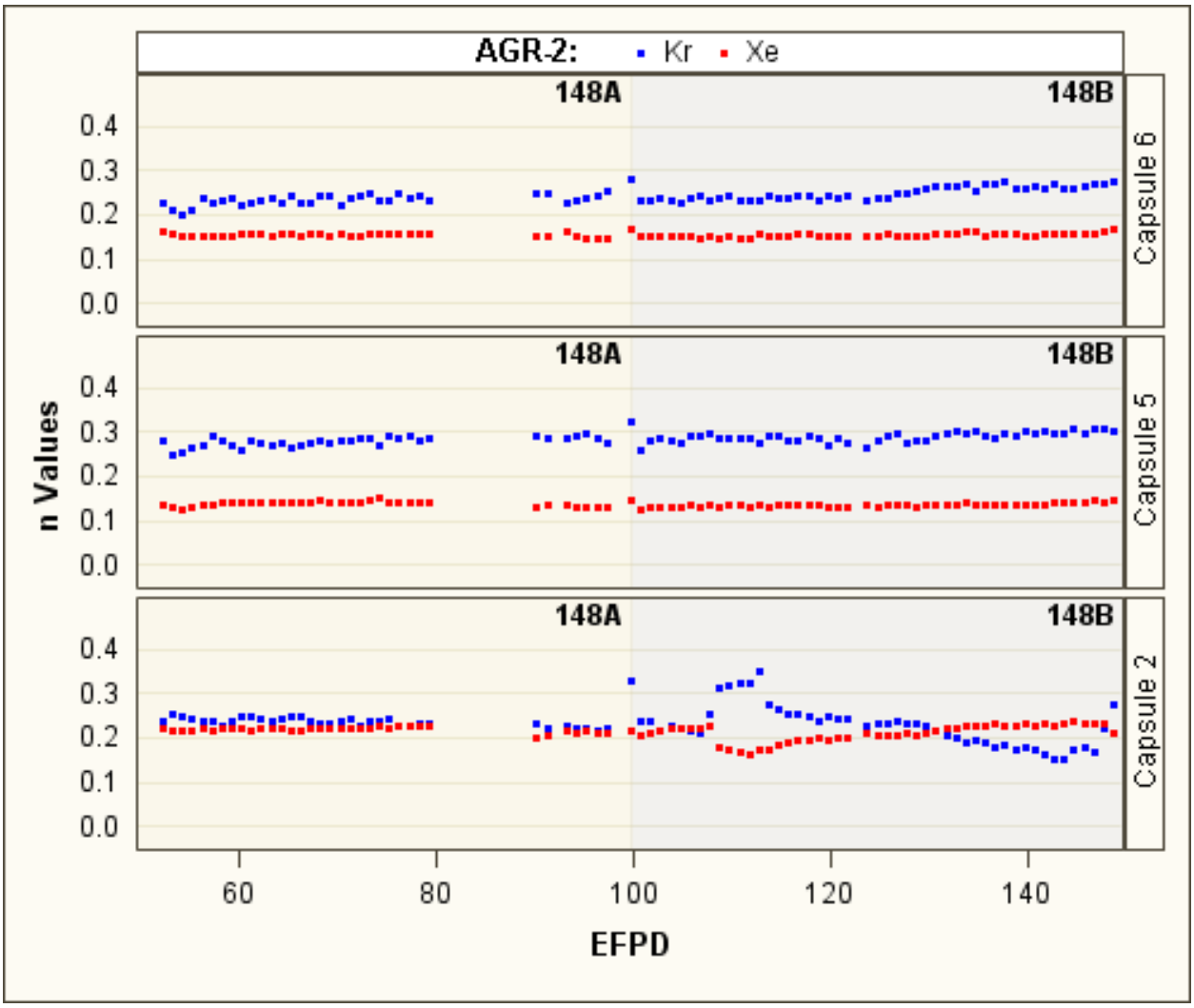

Figure 25. Krypton and xenon *n* values as a function of EFPD for AGR-2 U.S. UCO Capsules 2, 5, and 6.

4.2 Regression Analysis Results for Advanced Gas Reactor-3/4

Regression is performed to fit Equation 7 to daily averaged R/B per failed particle data obtained from the 12 AGR-3/4 capsules. The regression results discussed in the following subsections are obtained using fuel temperature in degrees Kevin and decay constants in s^{-1}.

4.2.1 Impact of Failure Count Uncertainty

To study the impact of the uncertainty of particle failure estimations on the release relationship as a function of fuel temperature and decay constants, the regressions were performed separately for three sets of R/B per failed particle calculated using the best-estimate, maximum, and minimum failure counts. Table 7 presents the three corresponding sets of parameter estimates (n, B, and C) of Equation 7 distinctly for krypton and xenon isotopes. As expected from the previous section, the *n* value for AGR-3/4 fuel particles is equal to approximately 0.3 for both the krypton and xenon isotopes, which is consistent with the calculated daily n values plotted in Figure 23 and Figure 24. Despite a large variation of the release data, there is a clear trend of temperature influence on R/B per failed particle as shown in Figure 26 for Kr-85m. However, the large variation of R/B for reciprocal temperature between 7.0E-4 and 7.5E-4 (R/B in Capsules 2, 4, 5, 6, and 9, with peak fuel temperature around 1100°C) and unexpected higher R/B in

Capsule 12 with the lowest peak fuel temperature lead to the 95% bounds (light blue area) around the fitted line.

Figure 26 shows AGR-3/4 R/B per failed particle and their fitted function of reciprocal peak fuel temperature for Kr-85m, using best-estimated (blue), maximum (red), and minimum (green) failure counts. The regression analysis results presented in Table 7 and Figure 26 indicate no significant impact of the failure count uncertainty on the regression fitting parameters because of the following observations:

1. The n value estimates are the same for all three data sets of R/B per failed particle for both krypton and xenon isotopes, reflecting the consistency of decay constant influence on release
2. Three fitted lines (blue, red, and green) are fairly parallel to each other, with a small shift indicating a small variation of parameter *B* estimates that reflect the consistency of temperature influence on release
3. The shaded area representing 95% confidence bounds on the fitted line using best-estimate failure counts covers most of the three sets of R/B per failed particle, indicating that variation due to failure count uncertainty is well within the variation of the large quantity of R/B data used in the fitting process.

In conclusion, the uncertainty of the failure counts does not affect *n* because it is defined mainly by fuel particle material properties. Additionally, estimates for the *B* parameter are similar for krypton and xenon isotopes also indicating the uncertainty of the failure counts does not affect the release correlation with temperature.

Table 7. Parameter estimates for AGR-3/4 R/B per failed particle data.

Isotopes	n	B	C
	Best-estimate number of failures		
Kr-85m Kr-87 Kr-88	0.327	-9118	-1.11
Xe-135 Xe-137 Xe-138	0.302	-8657	-2.19
	Maximum number of failures		
Kr-85m Kr-87 Kr-88	0.327	-9580	-1.02
Xe-135 Xe-137 Xe-138	0.302	-9119	-2.10
	Minimum number of failures		
Kr-85m Kr-87 Kr-88	0.326	-9548	-0.531
Xe-135 Xe-137 Xe-138	0.302	-9086	-1.61

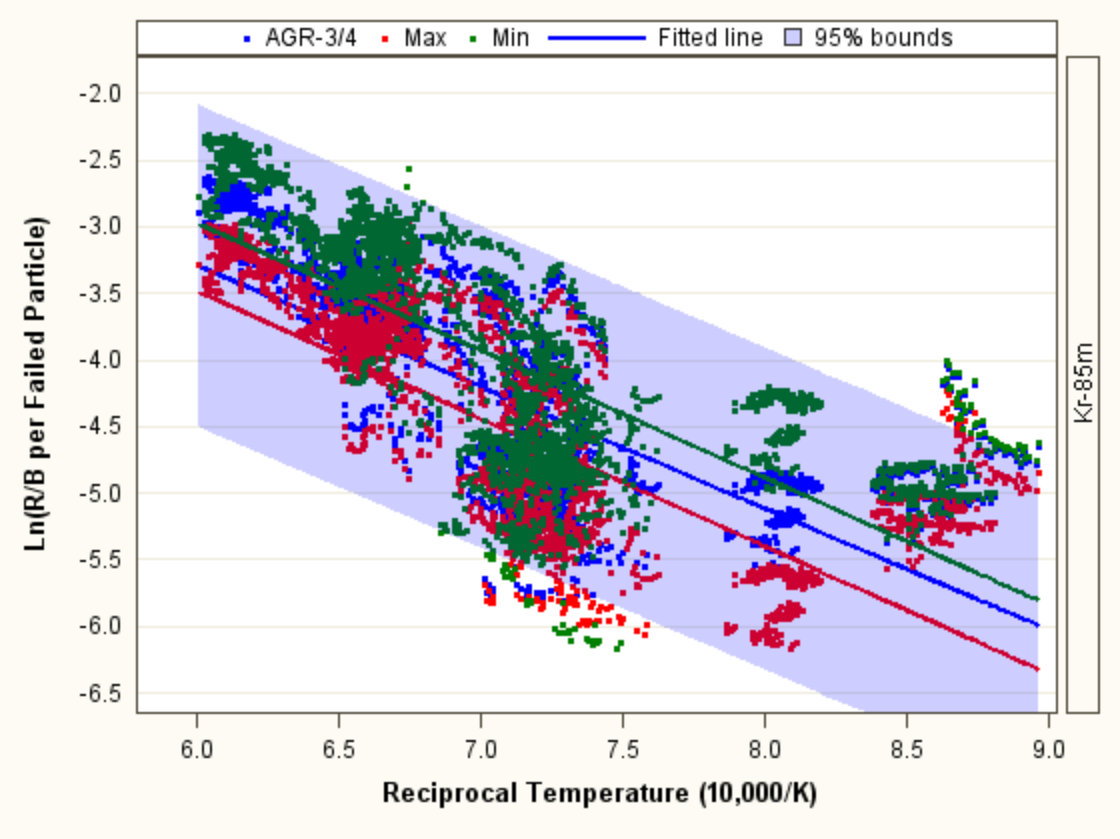

Figure 26. AGR-3/4 R/B per failed particle and their fitted function of reciprocal peak fuel temperature for Kr-85m using best-estimated, maximum, and minimum failure counts.

4.2.2 Regression Analysis Results

This section presents the results of regression fitting of R/B per failed particle that was calculated using the best-estimated failure counts for 12 AGR-3/4 capsules. The regressions were performed separately for the krypton and xenon isotopes. The parameter estimates (n, B, and C) were presented in the top section of Table 7. Additionally, estimates for Parameter *B* were similar for the krypton and xenon isotopes. However, estimates for Parameter *C* were much lower for the xenon isotopes, indicating their lower release.

In order to clearly show the data trend, Figure 27 depicts R/B per failed particle data and the fitted line in natural logarithm scale (top panel) and R/B per failed particle in linear scale (bottom panel) as a function of reciprocal fuel temperature for Kr-85m only. These plots are similar for the other five isotopes, which are plotted together in Figure 28 for krypton isotopes and Figure 29 for xenon isotopes. Note that the R/B data of the xenon isotopes are more scattered and significantly lower than the R/B data of the krypton isotopes.

The plots of R/B per failed particle in linear scale (bottom plots in Figure 27 through Figure 29) show that R/B per failed particle for both krypton and xenon isotopes are less than 1% and are not sensitive to fuel temperature when fuel temperatures are below 1050°C. However, when fuel temperature is greater than 1050°C, R/B increases exponentially (top plots) with increasing fuel temperature, which can be described by the model form in Equation 7. As a result, the clear downward trend of the fitted lines for R/B per failed particle and reciprocal fuel temperature confirms the exponential functional relationship for all isotopes.

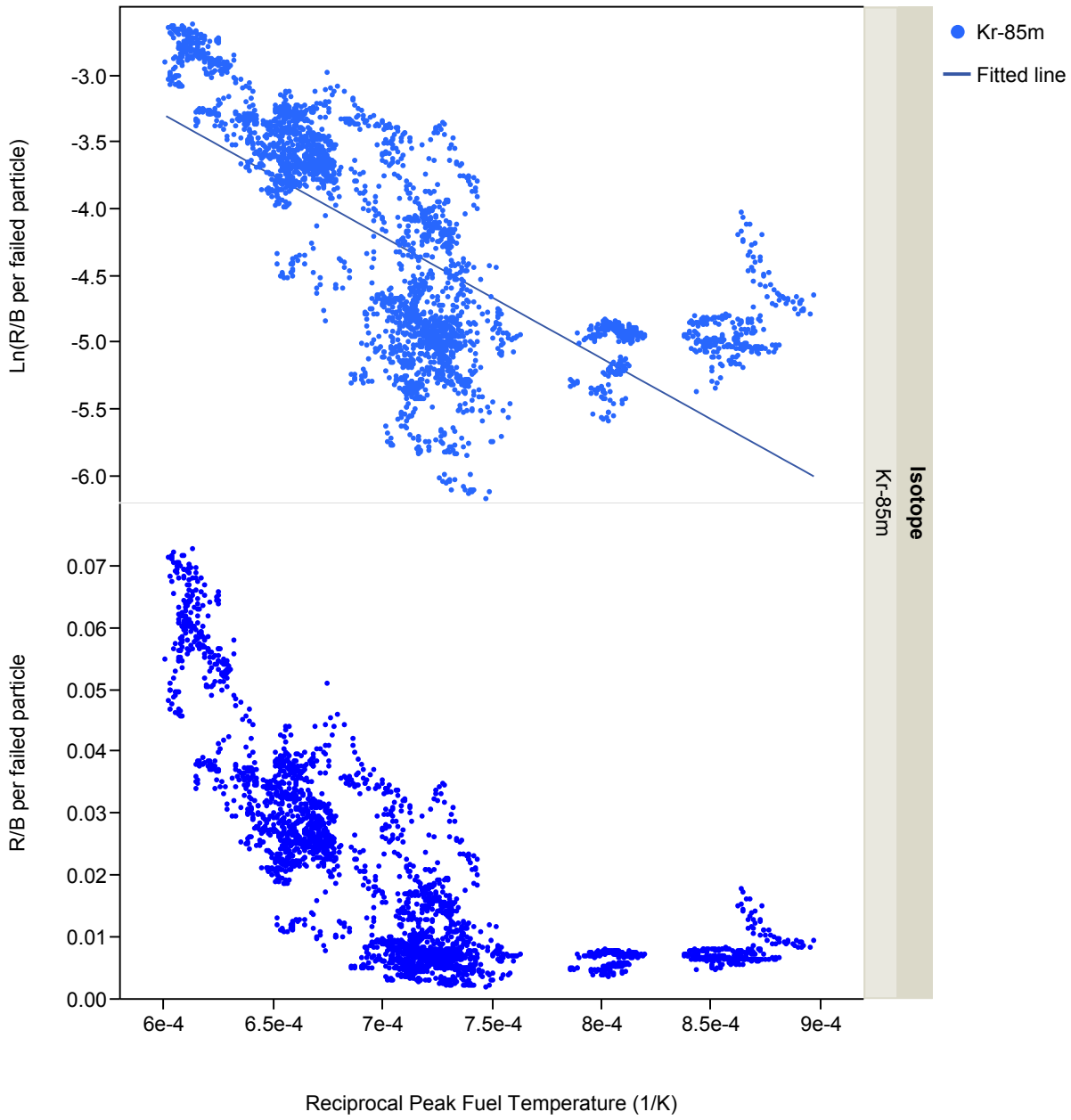

Figure 27. For Kr-85m (top panel) R/B per failed particle and the fitted line in natural logarithm scale and (bottom panel) R/B per failed particle in linear scale.

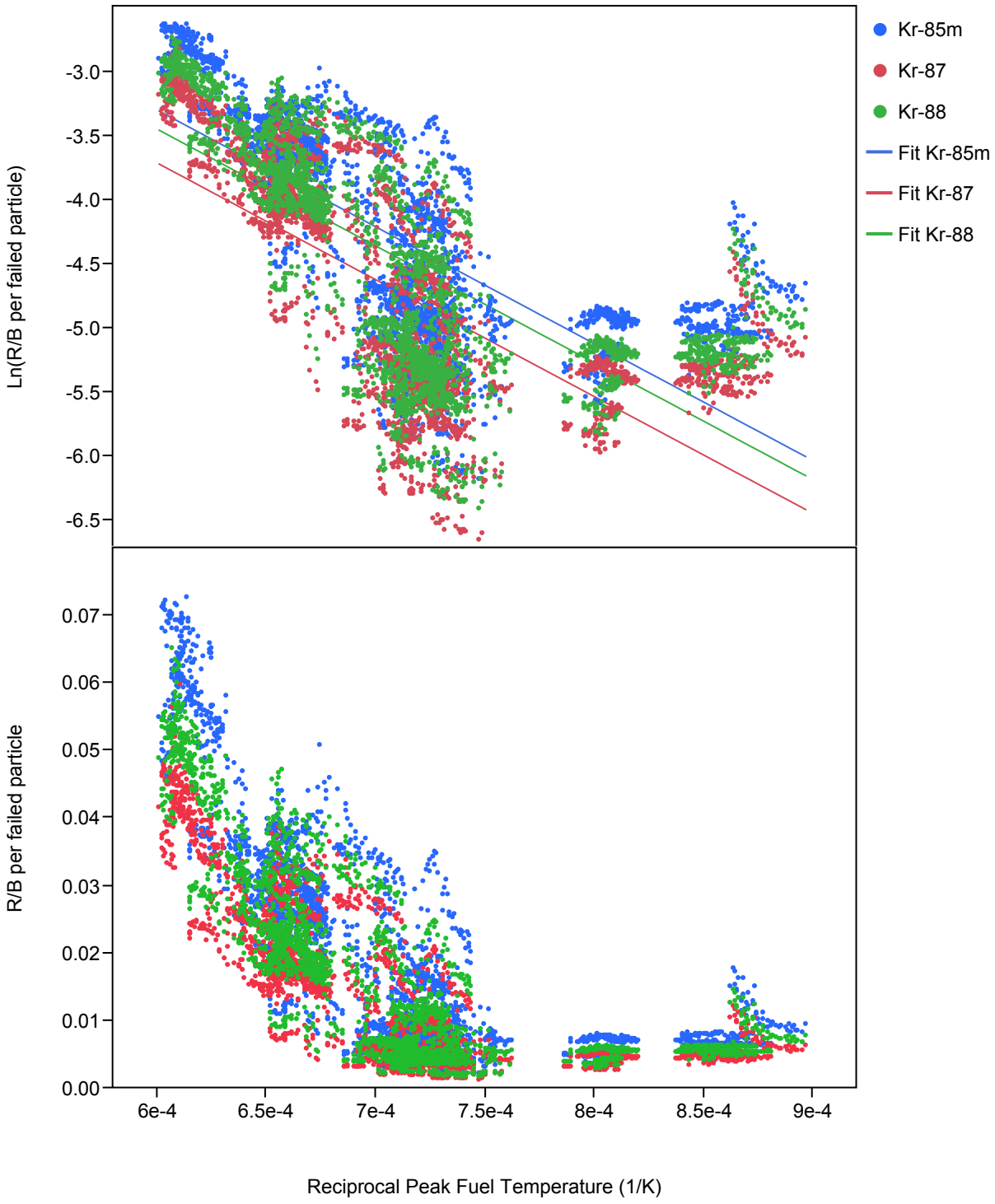

Figure 28. Krypton isotopes: (top panel) R/B per failed particle and the fitted line in natural logarithm scale and (bottom panel) R/B per failed particle in linear scale.

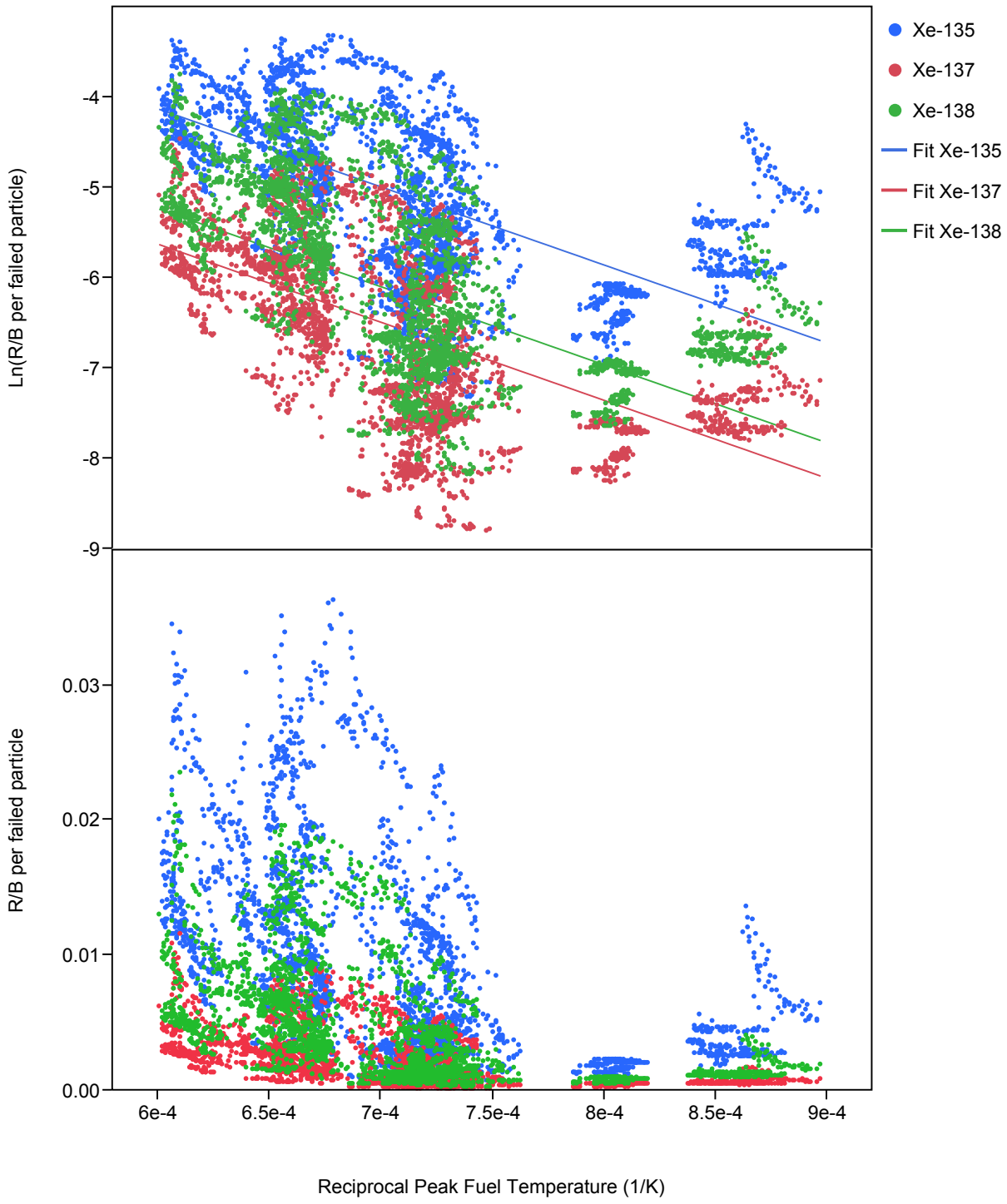

Figure 29. Xenon isotopes: (top panel) R/B per failed particle and the fitted line in natural logarithm scale and (bottom panel) R/B per failed particle in linear scale.

4.3 Release-to-Birth Ratio Data Comparison

4.3.1 Advanced Gas Reactor-2 and Advanced Gas Reactor-3/4 irradiations

Figure 30 shows the Kr-85m R/B per failed particle data for AGR-2 (red dots) and AGR-3/4 (blue dots) irradiations. This figure also presents the fitted line and 95% bounds for AGR-3/4 R/B data. The fact that AGR-2 R/B data lie completely within the 95% bounds of the fitted line for AGR-3/4 R/B data indicates excellent consistency between these two AGR irradiations. Furthermore, AGR-2 R/B data nicely filled in the gap in reciprocal fuel temperature between 7.4E-4 and 7.9E-4, where there are no AGR-3/4 R/B data. Consistency is also shown by the decrease in R/B data in the reciprocal temperature range of 6.8E-4 to 7.4E-4 for both AGR-2 and AGR-3/4.

Because of the excellent agreement between applicable R/B per failed particle data obtained during AGR-2 and AGR-3/4 irradiations, these data were combined in the regression fit to Equation 7. The combined parameter estimates are presented in the bottom panel of Table 8, along with parameter estimates using only AGR-3/4 irradiation data. The *n*, *B*, and *C* estimates are similar for both data sets (AGR-3/4 only and combined AGR-2 and AGR-3/4). This confirms the consistency between R/B data obtained from these two AGR irradiations.

Figure 31 (for krypton isotopes) and Figure 32 (for xenon isotopes) also show excellent agreement between R/B per failed particle data obtained during AGR-2 and AGR-3/4 irradiations for all six isotopes. AGR-2 R/B data (red dots) are blended and fill-in nicely with AGR-3/4 data (red dots). The combined fitted lines (purple lines) also fit well to R/B data of both AGR-2 and AGR-3/4 irradiations for all six isotopes. Because AGR-2 R/B per failed particle data are somewhat lower than AGR-3/4 R/B data, all combined parameter estimates are also slightly lower than parameter estimates for AGR-3/4 R/B data for both krypton and xenon isotopes (as shown in Table 8).

Table 8. Parameter estimates for AGR-3/4 data and for combined AGR-2 and AGR-3/4 R/B data.

Isotopes	n	B	C
	AGR-3/4 only		
Kr-85m Kr-87 Kr-88	0.327	-9118	-1.11
Xe-135 Xe-137 Xe-138	0.302	-8657	-2.19
	Combined AGR-3/4 and AGR-2		
Kr-85m Kr-87 Kr-88	0.319	-9023	-1.132
Xe-135 Xe-137 Xe-138	0.286	-8359	-2.288

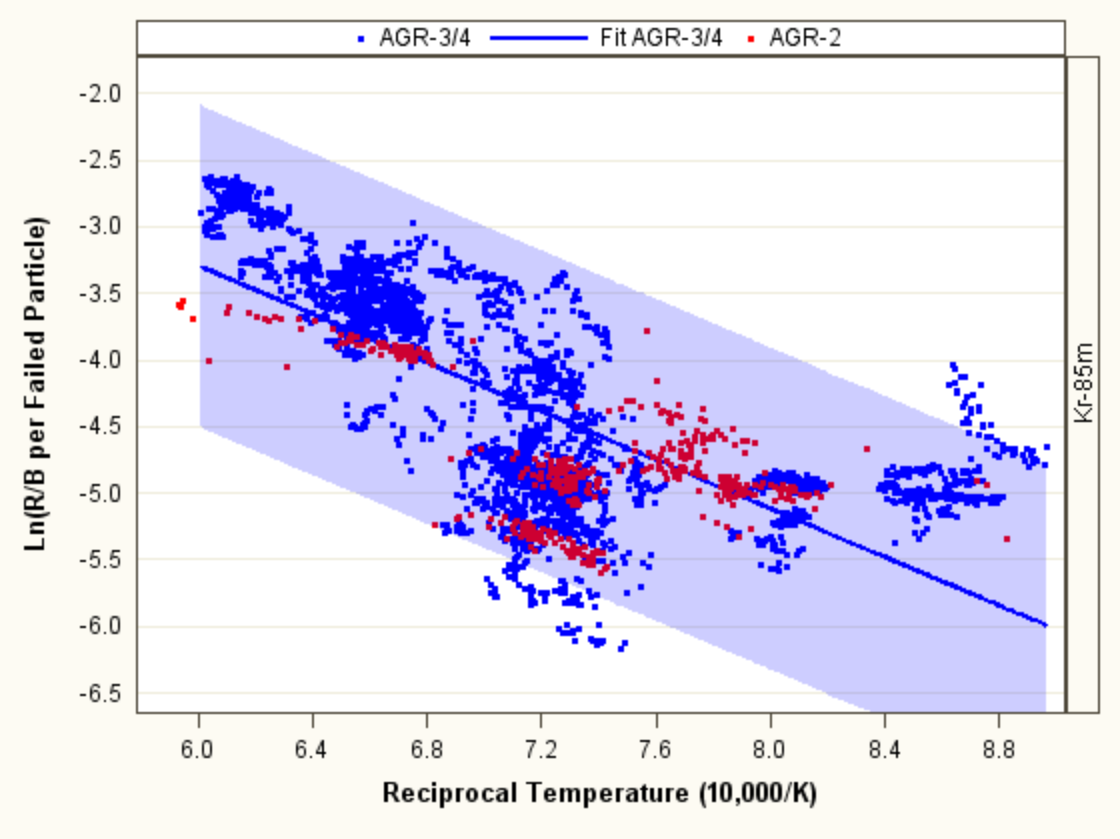

Figure 30. AGR-3/4 fitted line and experimental R/B per failed particle data plotted with AGR-2 data.

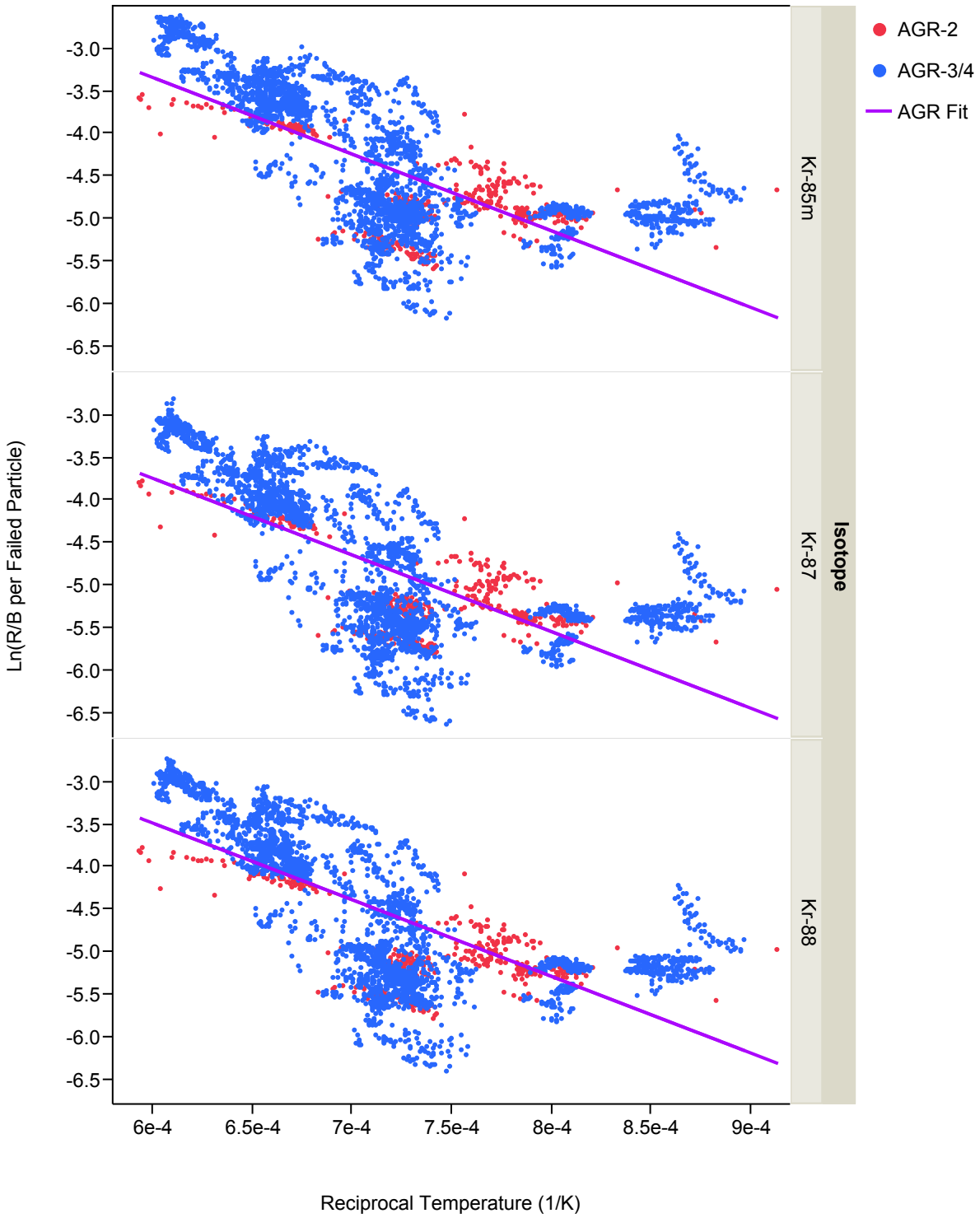

Figure 31. Combined fitted lines and krypton R/B per failed particle data from AGR-2 (red dots) and AGR-3/4 (blue dots) irradiations.

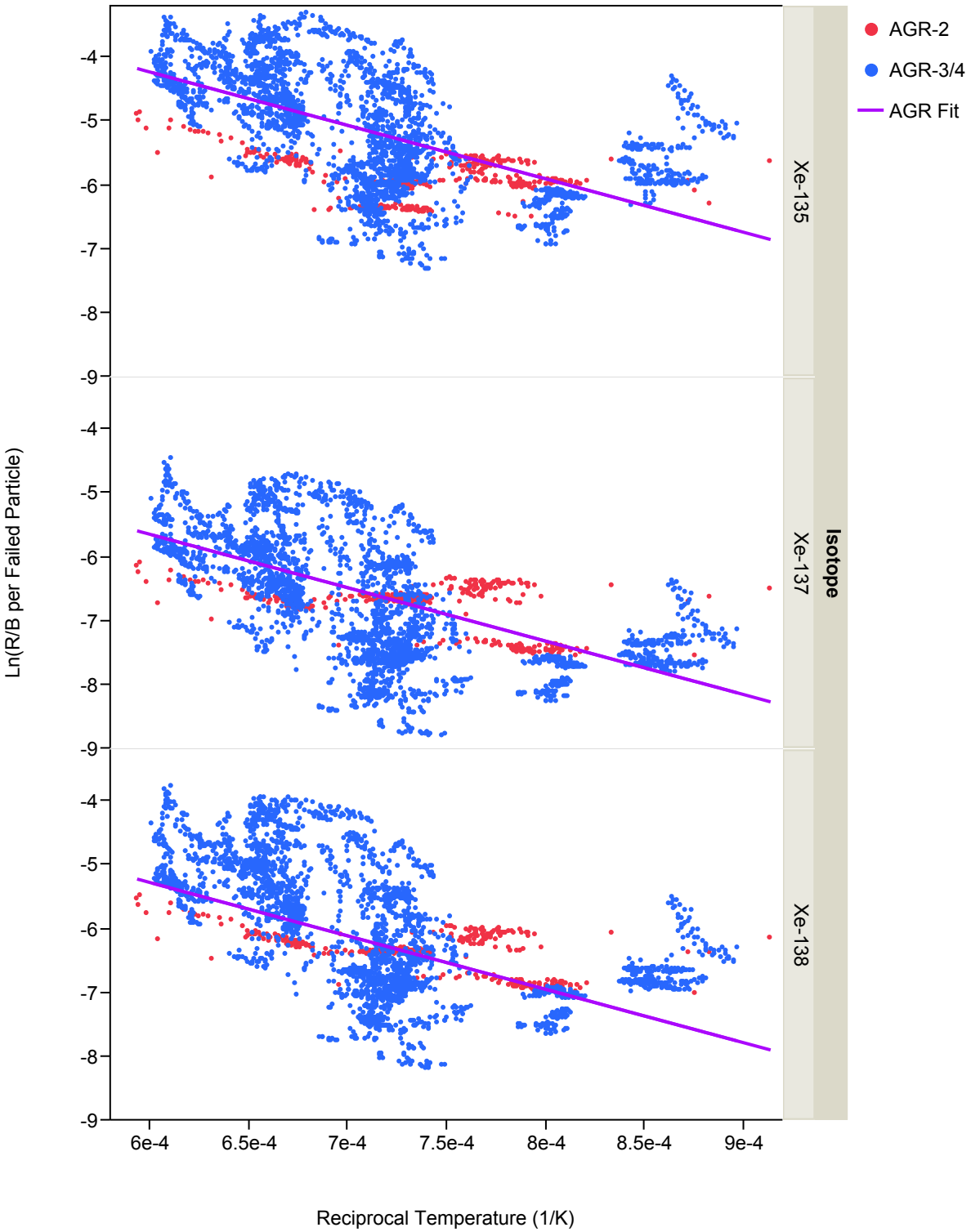

Figure 32. Combined fitted lines and xenon R/B per failed particle data from AGR-2 (red dots) and AGR-3/4 (blue dots) irradiations.

4.3.2 Advanced Gas Reactor and Historical Irradiations

Figure 33 shows R/B per failed particle data obtained from the two AGR irradiations, the four historical irradiations presented earlier, and two historical models. The German model is discussed in reference (IAEA 1997). The model developed by General Atomics is discussed in Richards report (Richards 1994). The fact that R/B per failed particle data from all historical irradiations lie well within the 95% bounds of the fitted line for the R/B data of AGR irradiations indicates good performance of AGR experiment fuel particles.

The German model (purple dashed line) is at the upper end of the AGR data range and the slope is very similar. The General Atomics model (orange dashed line) lies above the AGR fitted line and below the German model. The German and General Atomics models are conservative because they predict higher R/B per failed particle than the prediction of the model based on AGR-2 and AGR-3/4 data (i.e., the German model for the entire temperature range and the General Atomics model for lower temperatures). This is because these historical models were intentionally conservative.

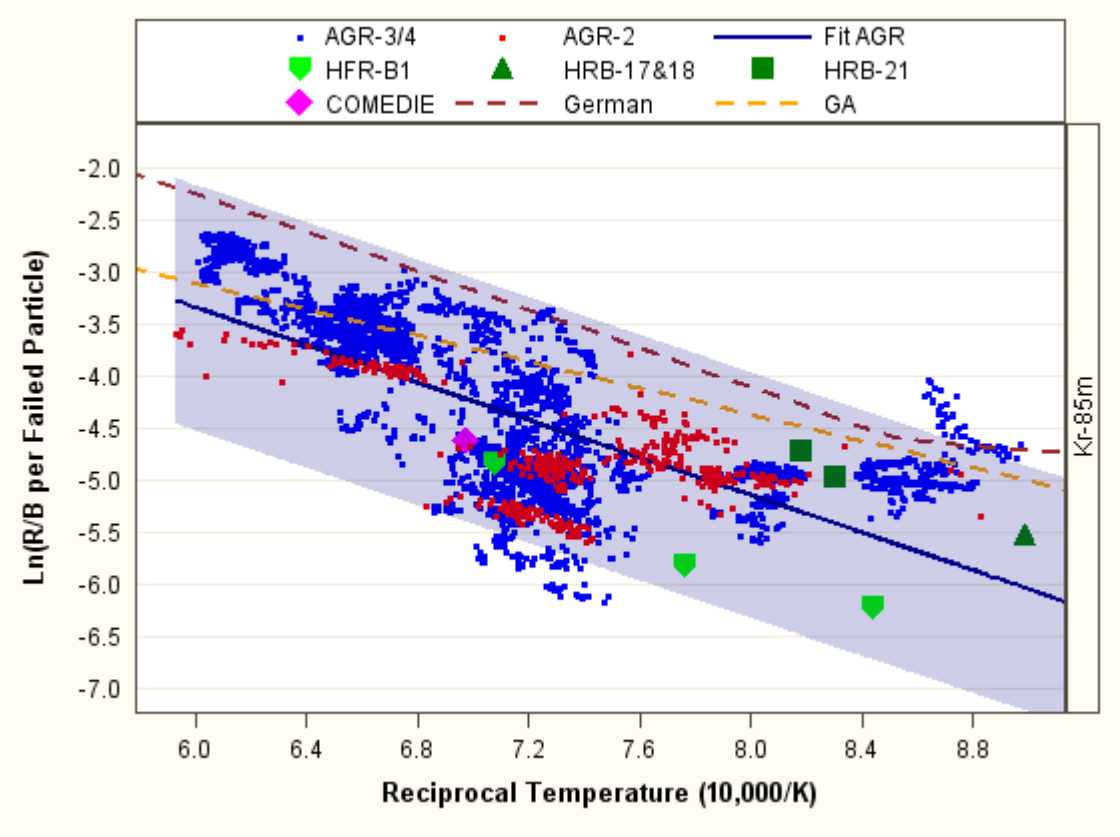

Figure 33. Combined AGR fitted line and R/B per failed particle data for AGR irradiations, historical irradiations, and models (the blue shaded area is 95% bounds of the fitted line).

5. CONCLUSION

To reduce measurement uncertainty of the release rate, the krypton and xenon isotopes selected for regression analysis have a short enough half-life to reach equilibrium in the capsule, but are also long enough to provide a measureable signal in the FPMS detector. These isotopes are Kr-85m, Kr-87, Kr-88, Xe-135, Xe-137, and Xe-138. Additionally, only AGR-2 and AGR-3/4 R/B data with measurement uncertainty less than 50% and standard 8-hour sampling durations are included in this analysis.

With embedded DTF fuel particles, AGR-3/4 irradiation provides invaluable R/B data for studying the fission product behavior of TRISO-coated UCO fuel. AGR-3/4 fuel particles were irradiated for 369.1 EFPDs and reached a peak burnup of 15.3%, a maximum fast neutron fluence accumulation of 5.3×10^{21} n/cm^2, and a peak fuel temperature ranging between 850 and 1450°C. A total of 18,479 daily values of AGR-3/4 R/B per failed particle for six selected krypton and xenon isotopes were used for this regression analysis. Even without DTF fuel particles included in capsules, the AGR-2 irradiation provides additional data for R/B per failed particle because exposed kernels existed in the test fuel that was irradiated. However, because of the relief valve issues and cross-talk failures, only 2,550 daily values of the AGR-2 R/B per failed particle during Cycles 148A and 148B were used for the regression analysis. For the AGR-3/4 irradiation, the krypton R/B per failed particle data vary widely in the range of 0.13 to 7.3% and the xenon R/B per failed particle data are somewhat lower and in the range of 0.015 to 3.6%. For the AGR-2 irradiation, the krypton R/B per failed particle data are in the range of 0.30 to 2.87% and xenon R/B per failed particle data are in the lower ranges of 0.09 to 0.77%. This large amount of R/B data combined from AGR-2 and AGR-3/4 irradiations allows assessment of the effect of isotopic decay constants and fuel temperatures on fission product releases.

The R/B correlation with isotopic decay constant is characterized by *n* values, which represent a slope between $\ln R_p$ and $\ln \frac{1}{\lambda}$ for isotopes of each gas element (e.g., krypton or xenon) and for constant fuel temperature. There is no effect of temperature on n values, because n values are similar across AGR-3/4 capsules, which have a wide range of fuel temperatures. The daily n values for AGR-2 and AGR-3/4 irradiations are about 0.3 and stable as a function of irradiation time, indicating no apparent effect of fuel burnup on fission product releases.

The R/B per failed particle for both krypton and xenon isotopes are less than 1% and not sensitive to fuel temperature when fuel temperatures are below 1050°C. However, when fuel temperature is greater than 1050°C, the R/B per failed particle values increase exponentially with increasing fuel temperature. The clear downward trend of the fitted lines for AGR-2 and AGR-3/4 R/B data confirms this exponential functional relationship between R/B per failed particle and reciprocal fuel temperature for all isotopes. The 95% confidence bands on the distribution are within a factor of 2.5 of the fitted value indicating the respectable consistency of R/B per failed particle data given high uncertainties in both fission product release measurement and particle failure estimation. These R/B correlations can be used by reactor designers to estimate fission gas release from postulated failed fuel in HTGR cores, which is the key safety factor for fuel performance assessment.

This analysis found that R/B data for AGR-2 and AGR-3/4 test fuel are consistent with each other and complementary. They are also comparable to R/B obtained in historic tests. The German and General Atomics models predict higher R/B per failed particle than the prediction of the model based on AGR-2 and AGR-3/4 data (i.e., the German model for the entire temperature range and the General Atomics model for lower temperatures. This is because these historical models were intentionally conservative.

6. REFERENCES

ANS, 2011, "American National Standard Method for Calculating the Fractional Release of Volatile Fission Products from Oxide Fuel," American National Standards Institute, Inc., ANSI/ANS-5.4-2011, May 2011.

ASME NQA-1-2008, "Quality Assurance Requirements for Nuclear Facility Applications," 1a 2009 addenda.

IAEA, 1997, "Fuel Performance and Fission Product Behaviour in Gas Cooled Reactors," IAEA-TECDOC-978, November 1997, http://www-pub.iaea.org/MTCD/Publications/PDF/te_978_prn.pdf.

Collin, B., 2011a, "AGR-2 Irradiation Experiment Test Plan," INL/PLN-3798, Revision 1, Idaho National Laboratory.

Collin, B., 2011b, "AGR-3/4 Irradiation Experiment Test Plan," INL/PLN-3867, Revision 0, Idaho National Laboratory.

DOE, 1995, "Fuel Capsule HRB-21 Post Irradiation Examination Data Report," DOE-HTGR-100229/ORNL-6836, April 1995.

Hawkes G., J. Sterbentz, and B. Pham, 2014a, "Thermal Predictions of the AGR-2 Experiment with Variable Gas Gaps," ANS2014, Reno, Nevada.

Hawkes, G. L. et al., 2014b, "Thermal Predictions of the AGR-3/4 Experiment with Time Varying Gas Gaps," 2014 ASME International Mechanical Engineering Congress & Exposition, Paper IMECE2014-36943, November 2014, Montreal, Canada.

Hunn J., 2010, "AGR-2 Fuel Compact Information Summary," ORNL/TM-2010/296, November 2010.

INL, 2014, "Technical Program Plan for the Very High Temperature Reactor Technology Development Office/Advanced Gas Reactor Fuel Development and Qualification Program," INL/PLN-3636, Revision 3, Idaho National Laboratory, May 2014.

General Atomics, 1987, "Capsule HRB-17/18 Data File," GA 1485, Revision 4.

General Atomics, 2009, "Technical Basis for NGNP Fuel Performance and Quality Requirements," GA Project 30302, Revision 0.

Martin, R. G., 1993, "Compilation of Fuel Performance and Fission Product Transport Models and Database for MHTGR Design," ORNL/NPR-91/6, October 1993.

McIsaac, C. V. et al., 1992, "Concentrations of Fission Product Noble Gases Released During the NP-MHTGR Fuel Compact Experiment-1A," ST-PHY-92-032, April 1992.

Mrowec, S., 1980, "Defects and diffusion in solids," Amsterdam-Oxford-New York.

NRC, 2004, "TRISO-Coated Particle Fuel Phenomenon Identification and Ranking Tables (PIRTs) for Fission Product Transport Due to Manufacturing, Operations, and Accidents," NUREG/CR-6844, Vol. 1-3.

ORNL, 1994, "The Operation of Experiment HFR-B1 in the Petten High Flux Reactor," ORNL/TM-12740, September 1994.

Pham, B. T. and J. J. Einerson, 2014, *AGR 2 Final Data Qualification Report for U.S. Capsules ATR Cycles 147A through 154B*, INL/EXT 14 32376, Idaho National Laboratory.

Richards, M. B., 1994, "Fission-Gas Release from UCO Microspheres: A Theoretical Model for Fractional Release for Non-hydrolyzed Fuel with Model Parameters Derived for Capsule HFR-B1," General Atomics, January 1994.

Scates, D. M., 2010, “Fission Product Monitoring and Release Data for the Advanced Gas Reactor -1 Experiment,” Paper 52, Proceedings HTR-2010, Prague, Czech Republic, October 18–20, 2010.

Scates, D. M., 2014a, “Release to Birth Ratios for AGR 2 Operating Cycles 147A through 154B,” ECAR 2420, Revision 0, Idaho National Laboratory, 2014.

Scates, D. M., 2014b, “Release-to-Birth Ratios for AGR3/4 Operating Cycles 151A-155A,” ECAR-2457, Idaho National Laboratory.

SPC-1064, “AGR-2 Irradiation Test Specification,” Rev. 1, Idaho National Laboratory, Idaho Falls, ID.

SPC-1345, “AGR-3/4 Irradiation Test Specification,” Rev. 1, Idaho National Laboratory, Idaho Falls, ID, Rev. 0, 2011.

Sterbentz, J. W., 2014, “JMOCUP As-Run Daily Depletion Calculation for the AGR-2 Experiment in ATR B-12 Position,” INL/ECAR-2066, Idaho National Laboratory.